Universal conditional knockout approach to multiple species, from fish to human induced pluripotent stem cells

Jung-Hwa Choi, Jihoon Moon, Youngchul Oh, Thomas M Klompstra, Yujin Kim, Gayoung Baek, Yejin Kwak, Yeongjun Kim, Sangmin Lee, Sujin Park, Jeongmin Ha, Ohbin Kwon, Young Ki Choi, Jeong Hun Kim, Ji-Hyun Lee, Jeongbin Park, Jong Kyoung Kim, Dong Ho Woo, Ki-Jun Yoon, Bon-Kyoung Koo, Heetak Lee

Nucleic Acids Research, 2026, **54**, gkag480
https://doi.org/10.1093/nar/gkag480
Data Resources and Analyses

OXFORD

Universal conditional knockout approach to multiple species, from fish to human induced pluripotent stem cells

Jung-Hwa Choi[1,#], Jihoon Moon[1,2,3,4,#], Youngchul Oh[1,5,#], Thomas M. Klompstra[1,2,$], Yujin Kim[1,$], Gayoung Baek[1,$], Yejin Kwak[6], Yeongjun Kim[1,7], Sangmin Lee[1,7], Sujin Park[1], Jeongmin Ha[1], Ohbin Kwon[1,8], Young Ki Choi[9], Jeong Hun Kim[10], Ji-Hyun Lee[1], Jeongbin Park[6], Jong Kyoung Kim[5], Dong Ho Woo[3,4,*], Ki-Jun Yoon[2,8,*], Bon-Kyoung Koo[1,3,8,*], Heetak Lee[1,*]

[1]Center for Genome Engineering, Institute for Basic Science (IBS), Expo-ro 55, Yuseong-gu, Daejeon 34126, Republic of Korea
[2]Department of Biological Science, Korea Advanced Institute of Science and Technology (KAIST), Daejeon 34141, Republic of Korea
[3]Center for Global Pharmaceutical and Bio Research Center, Korea Institute of Toxicology (KIT), Daejeon 34114, Republic of Korea
[4]School of Korea Institute of Toxicology, University of Science and Technology, 34113 Daejeon, Republic of Korea.
[5]Department of Life Sciences, Pohang University of Science and Technology (POSTECH), Pohang 37673, Republic of Korea
[6]Department of Information Convergence Engineering, Pusan National University, Yangsan 50612, Republic of Korea
[7]Department of Biology, College of Science, Kyung Hee University, Seoul 02453, Republic of Korea
[8]Graduate School of Stem Cell and Regenerative Biology, Korea Advanced Institute of Science and Technology (KAIST), Daejeon 34141, Republic of Korea
[9]Center for Study of Emerging and Re-emerging Viruses, Korea Virus Research Institute, Institute for Basic Science (IBS), Daejeon 34126, Republic of Korea
[10]Fight against Angiogenesis-Related Blindness (FARB) Laboratory, Biomedical Research Institute, Seoul National University Hospital, Seoul 03080, Republic of Korea

*To whom correspondence should be addressed. Email: leeheetak@ibs.re.kr
Correspondence may also be addressed to Bon-Kyoung Koo. Email: koobk@ibs.re.kr
Correspondence may also be addressed to Ki-Jun Yoon. Email: kijunyoon@kaist.ac.kr
Correspondence may also be addressed to Dong Ho Woo. Email: DongHo.woo@kitox.re.kr
#These authors contributed equally.
$These authors contributed equally.

Abstract

Investigating essential gene function in vertebrate development and disease is challenging due to associated lethality, necessitating precise conditional inactivation. While existing conditional knockout methods can be inefficient and demanding, especially in models like zebrafish and human induced pluripotent stem cells (iPSCs), a widely applicable system has remained elusive. Here, we demonstrate the expanded utility and versatility of a Short Conditional intrON (SCON) knockout cassette, now validated for efficient conditional loss-of-function mutation generation in diverse vertebrate models, including zebrafish, human iPSCs, and intestinal organoids. Building on this validated broad applicability, we establish a comprehensive, user-friendly web-based GenPos-SCON database (https://genpos.org/) to streamline conditional knockout design for over 300 vertebrate species. This powerful resource and proven methodology significantly accelerate systematic gene functional studies across the vertebrate tree, providing an unprecedented tool for dissecting fundamental biological processes and disease mechanisms in relevant contexts.

Received: September 23, 2025. **Revised:** April 17, 2026. **Accepted:** April 21, 2026

Graphical abstract

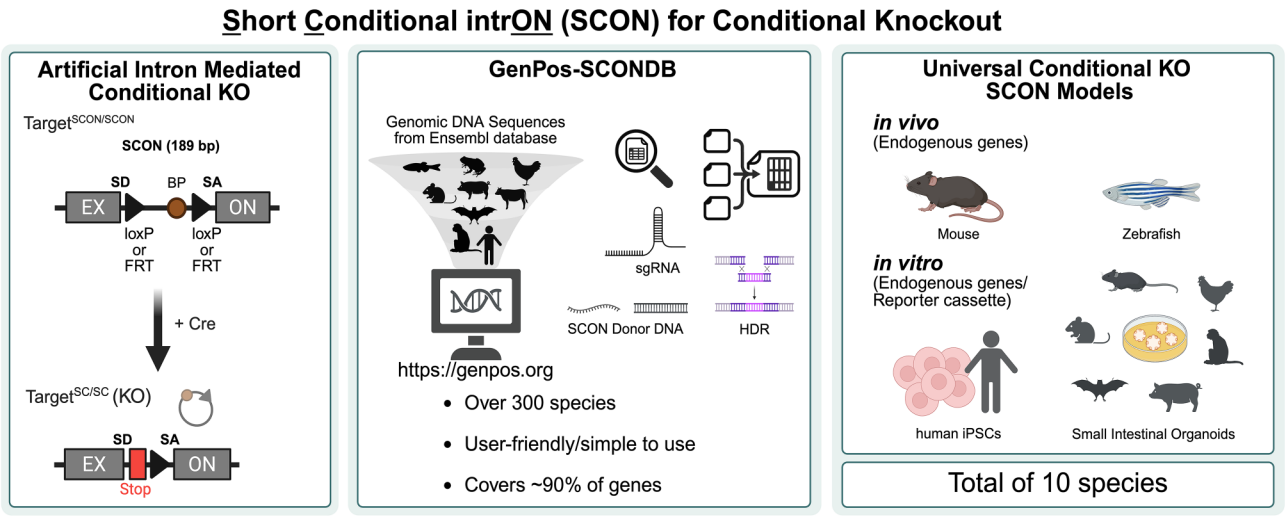

Introduction

Conditional knockout (cKO) methods are readily established for use in mice [1], yet they have not been widely adopted in other vertebrate models, causing technical limitations in working with species such as non-human primates [2]. Zebrafish, a popular model organism, lacks robust cKO capabilities. This causes researchers to often rely on traditional knockouts or morpholinos, which have inadequate precision and control compared to cKO for genetic studies [3]. Similarly, in human models, including induced pluripotent stem cells (iPSCs) [4] and stem cell-derived organoids, cKO remains technically complex, time-consuming, and costly, limiting its accessibility and practical application in disease modeling and developmental studies. Particularly, one-step homozygous conditional gene inactivation in iPSCs remains challenging for genes essential to embryonic development and cell survival. Existing obstacles with the conventional conditional knockout approach include low efficiency in integrating donor DNA at two target sites flanking an essential exon *in cis*, and difficulties in achieving these precise edits in both alleles simultaneously [5]. There is a pressing need for a broadly applicable, easy-to-use conditional knockout tool that can be used across multiple species.

Recently introduced intron-mediated conditional knockout strategies [6–12] are advantageous due to requiring integration of only a singular artificial Short Conditional intrON (SCON) for generating a conditional allele [9]. Once integrated, the expression of the target gene remains unperturbed until the excision of the intronic sequence by Cre or Flp recombinases [9, 10]. This SCON-based approach has the potential to greatly expand the use of conditional knockout approaches across various vertebrate models. However, its versatility has not been shown in species other than mice [9]. In this study, we explored the functionality of SCON in zebrafish and human iPSCs with endogenous gene targets, the GenPos-SCONDB (https://genpos.org/)-derived designs covering more than 300 species for SCON application, and intestinal organoids from various species to determine its potential as a robust and accessible method across multiple species.

Materials and methods

Mice

The mice were maintained separately in a specific pathogen-free (SPF) facility under a 12 h light/dark cycle. C57BL/6J and ICR mouse strains were used as embryo donors and foster mothers, respectively. The use of the mouse was approved by the Institutional Animal Care and Use Committee (IACUC) of the Institute of Basic Science [Protocol # IBS-2023–001].

Generation of SCON mouse

All SCON lines were generated via microinjection into one-cell-stage embryos. The CRISPR/Cas9 injection mix was prepared in nuclease-free TE buffer and consisted of spCas9 protein (30 ng/μl, Cat# 10 007 807, IDT), sgRNA (30 ng/μl, IDT), and ssODN (20 ng/μl, GenScript, Supplementary Table S7). The mixture was filtered with Spin-X® centrifuge tube filters (Cat# 8160, Corning) at 13 000 rpm at 4°C for 2 min to prevent the clogging of the injection needles.

Zebrafish husbandry

Zebrafish were maintained at 28°C in a recirculating system with dechlorinated water (system water) with 14 h of light and 10 h of dark cycles. We conducted our experiments using zebrafish from wild-type stocks with the AB genetic background [13], as well as the *Tg (hsp70l:Cre)*^{icf5} strain, also referred to as *hsp70:Cre*. The use of zebrafish was approved by the Institutional Animal Care and Use Committee (IACUC) of the Institute of Basic Science [Protocol # IBS-2025–018].

Production of sgRNAs and Cas9 mRNA for zebrafish

We selected sgRNA candidates using both GenPos-SCONDB (https://genpos.org/) and CRISPOR (http://crispor.gi.ucsc.edu/) [14], and produced the sgRNA template using a cloning-free approach described by Varshney *et al.* [15]. The oligo included the T7 promoter, a 20-nt target sequence, and a 20-nt sequence corresponding to a generic sgRNA template, according to Varshney *et al.* [15]. The sequence for the forward oligo is as follows (Macrogen,

Inc): 5′-TAATACGACTCACTATA-GGN-(18–20 nt target sequence)-GTTTTAGAGCTAGAAATAGC-3′. The targeting (forward) oligo was annealed with an 80-nt chimeric sgRNA core sequence (reverse oligo): (5′-AAAAGCACCG ACTCGGTGCCACTTTTTCAAGTTGATAACGGACTAG CCTTATTTTAACTTGCTATTTCTAGCTCTAAAAC-3′). The annealed oligos were then extended using Phusion DNA polymerase (New England BioLabs) under the following conditions: 98°C for 3 min; ramp down at 0.1°C/s to 50°C; 72°C for 30 min. The sgRNAs were synthesized using the MAXIscript™ T7 Transcription Kit (Cat # AM1312, Thermo Fisher Scientific). To produce Cas9 mRNA, the pT3Ts *nCas9n* (Addgene, plasmid #46 757) [16] template DNA was digested with XbaI, followed by synthesis using the mMESSAGE mMACHINE T3 Transcription Kit (Cat # AM1348, Thermo Fisher Scientific). Both sgRNAs and Cas9 mRNA were purified with Monarch® RNA Cleanup Kit (Cat # T2040L, New England BioLabs).

Construction of hsp70l:Cre

The *hsp70l:Cre* construct was cloned by combining the *hsp70l* fragment (Addgene plasmid #24 334) [17] and *Cre.zf1* fragment (Addgene plasmid #61 391) [18] in a *pDEST Tol2* vector (Addgene plasmid #81 181) [19] using the NEBuilder HiFi assembly master mix (Cat# N26611A, New England BioLabs), according to the manufacturer's protocol. The primers used were listed in Supplementary Table S5.

Microinjection and genotyping

To generate SCON zebrafish, a solution containing sgRNA for the target gene (∼50 ng/μl), Cas9 mRNA (∼500 ng/μl), and ssODN (∼20 ng/μl, GenScript, Supplementary Table S7), and phenol red (0.5%) was microinjected into the one-cell stage of zebrafish embryos, which were then raised to adulthood. We first performed a genotyping prescreening on fin samples from adult founder fish to identify the SCON-integrated founder, which was later confirmed in the F1 offspring embryos. The samples were lysed in 45 μl of 50 mM NaOH for 20 min at 95°C, followed by the addition of 5 μl of 1 M Tris-HCl (pH 8.0). After centrifugation at 14 000 rpm for 5 min, the supernatant was used for PCR genotyping (PCR parameters: 98°C for 3 min, followed by 32 cycles of denaturation at 98°C for 10 s, annealing at 59°C for 15 s, extension at 72°C for 30 s per kb, and a final extension step of 5 min at 72°C) with the primers listed in Supplementary Table S5. Sanger sequencing was subsequently conducted.

Generation of hsp70l:Cre transgenic line by Tol2 transgenesis

To produce Tol2 transposase mRNA, the *pT3TS_Transposase* (Addgene plasmid #109 768) [20] plasmid was digested with XbaI, and RNA was synthesized using the mMESSAGE mMACHINE T3 Transcription Kit (Cat # AM1348, Thermo Fisher Scientific) and purified with Monarch® RNA Cleanup Kit (Cat # T2040L, New England BioLabs). A solution containing *hsp70l:Cre* plasmid DNA (∼25 ng/μl), transposase (∼25 ng/μl), and phenol red (0.5%) was injected into one-cell stage zebrafish embryos, which were raised to adulthood. To identify transgenic founders, F0 adult fish were outcrossed to AB, and genomic DNA was extracted from pools of 10–50 outcrossed embryos collected at 2 dpf. The samples in lysis buffer (1.5 mM $MgCl_2$, 6 mM Tris Base, 4 mM Tris–HCl, 50 mM KCl, 0.3% Tween 20, and 0.3% NP-40) were heated to 95°C for 10 min. After cooling the samples on ice, 2.5 μL of Proteinase K solution (20 mg/mL, Cat # PR003S, Enzynomics) was added. The mixture was then incubated at 55°C for 1 h. To inactivate the Proteinase K, the samples were heated to 95°C for 10 min, followed by centrifugation at 14 000 rpm for 5 min. The supernatant was used for PCR genotyping and Sanger sequencing.

Cre mRNA and heat treatments

The *pCS2-Cre.zf1* (Addgene plasmid #61 391) [18] plasmid DNA was linearized by KpnI and synthesized using the mMESSAGE mMACHINE SP6 Transcription Kit (Cat # AM1340, Thermo Fisher Scientific), and purified with Monarch® RNA Cleanup Kit (Cat # T2040L, New England BioLabs), according to the manufacturer's instructions. Cre mRNA was injected into the SCON-positive progeny at the one-cell stage.

For heat treatment, undechorionated embryos (4 hpf from $sox2^{SCON}$) were transferred into fresh petri dishes, and the excess embryo medium was removed. Preheated embryo medium at 38°C was then added, and the dishes were incubated at 38°C for 1 h before being returned to a 28°C incubator.

RT-PCR

The total RNA was extracted from half of the zebrafish embryos at 3 dpf using TRIzol (Cat # 15–596-026, Ambion), then precipitated with isopropanol, and subsequently washed with 70% ethanol. The RNA was treated with DNase I (Cat # AM2238, Thermo Fisher Scientific) for 30 min at 37°C and purified with the Monarch® RNA Cleanup Kit (Cat # T2040L, New England BioLabs). For cDNA synthesis, 500 ng of total RNA was used according to the manufacturer's instructions with the EcoDry cDNA synthesis kit (Cat # 639 543, TaKaRa). RT-PCR was conducted with the primers listed in Supplementary Table S5 and the PrimeSTAR® GXL Premix (Cat# R051B, TaKaRa). The PCR conditions included an initial denaturation at 98°C for 3 min, followed by 27 cycles of denaturation at 98°C for 10 s, annealing at 59°C for 15 s, extension at 72°C for 30 s per kb, and a final extension step of 5 min at 72°C. Sanger sequencing was subsequently conducted. The total RNA was extracted from iPSCs with RNeasy Kit (Cat # 74 134, QIAZEN), and cDNA synthesis was subsequently done with PrimeScrip RT Master Mix (Cat # RR036A, TaKaRa) following the manufacturer's instructions. RT-PCR was conducted with GXL polymerase (Cat # R050A, TaKaRa).

Microscopy for zebrafish

The dechorionated embryos were mounted in 3% methylcellulose. A Nikon stereomicroscope (SMZ18) equipped with a digital camera (DS-Ri2) was used for low-magnification imaging.

Cell culture and maintenance of human iPSCs

The GM25256 iPSCs were obtained from the Coriell Institute for Medical Research and used as healthy controls. The iPSCs were maintained using StemFlex medium (Cat# A3349401, Gibco) containing antibiotic-Antimycotic (Cat# 15 240 062, Gibco) on plates coated with Matrigel® hESC-Qualified

Matrix (Cat# 354 277, Corning) and incubated at 37°C in a 5% CO_2 environment. To prepare the Matrigel coating, plates were incubated for at least 1 h with a 1% Matrigel solution in DMEM/F12 (Cat#11 320 033, Gibco) at 37°C. iPSCs were manually detached using ReLeSR (Cat# 100–0483, STEMCELL Technologies) according to the manufacturer's instructions. Karyotyping verified that the iPSCs exhibited a normal chromosomal profile.

Generation of a lentiviral vector and transduction

To validate the SCON cassette in iPSCs, the LV-CreERT2-2A-GFP vector and lentivirus were produced by the Virus facility at the Institute for Basic Science (IBS) in Korea. Twenty-four hours after transduction, the media were changed with fresh media, and single clone isolation was performed prior to validation.

Transfection into the human iPSC line and single clone isolation

To transfect iPSCs with CRISPR/Cas9 RNP and ssODN or plasmid, electroporation was performed using the NEPA21 device (NEPA GENE Co. Ltd.) according to the manufacturer's instructions. The cells were washed with DPBS, dissociated into single cells using Accutase (Cat # A1110501, Gibco) for 10 min at 37°C, and centrifuged at 1200 rpm for 3 min.

For electroporation, 1×10^6 cells were suspended in 100 μl of Opti-MEM™ (Cat# 31 985 062, Gibco) containing either 2 μg plasmid or Alt-R™-S.p.Cas9 nuclease V3 (10 μg, Cat# 1 081 059, IDT), Alt-R™ CRISPR-Cas9 crRNA (370 μM, IDT), Alt-R® CRISPR-Cas9 tracrRNA (370 μM, IDT) and donor DNA. For the SCON cassette knock-in, the donor DNA was used either ssODN (1 μg, GenScript, Supplementary Table S7) or dsDNA (1 μg, Twist Bioscience, Supplementary Table S7). After electroporation, cells were incubated with the StemFlex containing RevitalCell supplement (Cat# A2644501, Gibco) for 48 h.

For eG-SCON-FP reporter overexpression, electroporation was performed with a total of 5 μg DNA, consisting of 2 μg mCherry control plasmid and 3 μg of either empty, GFP, eG-SCON-FP, or eG-SC-FP vector.

For PB-eG-SCON-FP iPSCs generation, cells were transfected with PB-eG-SCON-FP (Supplementary Table S7) and PB Transposon plasmids [9]. A few days later, GFP^+ colonies were manually selected under the EVOS M7000 microscope. To test the functionality of the eG-SCON-FP cassette, the mCherry-IRES-Cre plasmid (Addgene #55 632) [21] was transfected and tested. Flow cytometry was performed using a BD LSRFortessa flow cytometer (BD Biosciences) in the IBS Research Solution Center (RSC). The mCherry fluorescence was excited with a 561 nm laser and detected through an mCherry bandpass filter installed in the PE detector position. The main cell population was gated on FSC/SSC, and single cells were gated by FSC-A and FSC-H. Subsequently, each population was analyzed as a contour plot by setting the Y-axis to PE-594-Am for mCherry and the X-axis to FITC-A for GFP. Flow cytometry analysis was conducted using FlowJo v10 software.

For isolating a single clone after CAG-GFP-IRES-Cre (Addgene #48 201) [22] transfection, GFP^+ iPSCs were sorted with MoFlo Astrios (Beckman Coulter Life Sciences).

For SCON knock-in iPSCs, cells were seeded onto 100 mm dishes at a limiting dilution to obtain single-cell-derived clones with RevitaCell (Cat # A2644501, Gibco) and StemFlex (Cat # A3349401, Gibco). After three days of incubation, the media was replaced with StemFlex until the clones reached an appropriate size for clonal isolation. In approximately 10 days, the colonies grew to a sufficient size (∼1 mm) for clonal isolation. At this stage, individual colonies were manually picked, with half of each colony placed into separate wells of a 96-well plate to establish clonal cell lines. The remaining colonies underwent genotyping analysis, such as PCR and Sanger sequencing, to confirm the successful integration of the SCON cassette at the targeted locus. Clones with the desired genotype were selected for further applications.

Genotyping and Sanger sequencing for iPSCs

To identify SCON cassette knock-in clones, isolated colonies from each clone were lysed using QuickExtract DNA Extraction Solution (Cat# QE09050, Biosearch Technologies). The extracted genomic DNA was then amplified by PCR using GXL polymerase (Cat # R050A, TaKaRa) and specific primers for each target, as listed in Supplementary Table S6. The PCR products from each colony were run on an agarose gel through electrophoresis, and genotyping was determined based on the size of the amplicons. To verify the integrated sequence at the target loci, the PCR products were purified and confirmed via Sanger sequencing.

Immunochemistry

iPSCs were plated on Matrigel-coated 4-well chamber slides. After 24 h of treatment with 0.5 μM 4-hydroxytamoxifen (4-OHT, Cat # H7904, Sigma-Aldrich), the cells were washed once with 1X PBS, followed by fixation with 4% paraformaldehyde at room temperature for 10 min. The fixed cells were then washed twice with 1X PBS and permeabilized for 10 min using 1X PBS containing 0.5% Triton-X-100 and 3% bovine serum albumin. Subsequently, the samples were incubated overnight at 4°C with primary antibodies: rabbit anti-YTHDC1 (1:400, Cat# 122 340, Abcam), mouse anti-CTNNB1 (1:400, Cat# 610 154, BD Biosciences), rabbit anti-SLC35A2 (1:100, Cat# 222 854, Abcam), and rabbit anti-Cleaved Caspase-3 (1:400, Cat# 9661, Cell Signaling Technology). The samples were washed twice with 1X PBS and incubated for 3–4 h at room temperature with 1X PBS containing Alexa Fluor 488 Donkey anti-rabbit (1:400, Cat # 711–545-152, Jackson ImmunoResearch), Alexa Fluor 594 Donkey anti-rabbit (1:400, Cat # 711–585-152, Jackson ImmunoResearch), and Alexa Fluor 488 Donkey anti-mouse (1:400, Cat # 715–545-150, Jackson ImmunoResearch) secondary antibodies. Afterward, the samples were washed twice with 1X PBS and incubated with 2 μg/ml DAPI in 1X PBS for 10 min before being mounted. Mounting was performed using VECTASHIELD® Antifade Mounting Medium (Cat # H-1000–10, Vector Laboratories, Inc.), and imaging was conducted using a Carl Zeiss LSM 800 confocal microscope.

MTT assay

Cell growth curve was assessed using the MTT (3- (4,5-dimethylthiazol-2-yl)-2,5-diphenyltetrazolium bromide) Assay Kit (Abcam, ab211091) according to the manufacturer's instructions. iPSCs were dissociated using a releaser and seeded in 96-well plates manually before assay. The assay was performed daily for four consecutive days, with four indepen-

dent samples for each group. Absorbance was measured at 590 nm using a microplate reader.

Bulk RNA-seq sample preparation and data analysis

iPSCs were plated on Matrigel-coated plates and treated with 0.5 μM 4-hydroxytamoxifen (4-OHT; Cat# H7904, Sigma-Aldrich) for 24 or 48 h. Total RNA was extracted using the RNeasy Mini Kit (Cat#74 104, Qiagen) according to the manufacturer's protocol. Sample libraries were prepared using the NEBNext Ultra™ II RNA Library Prep Kit for Illumina (Cat# E7770, NEB) and the Dynabeads mRNA DIRECT Kit (Cat# 61 012, Invitrogen), according to the manufacturers' instructions.

RNA-seq data were analyzed using the nf-core/rnaseq pipeline (v3.22.2) [23] with default settings. The quality of input FASTQ files was evaluated with FastQC (v0.12.1) (https://www.bioinformatics.babraham.ac.uk/projects/fastqc/), and adapter sequences were trimmed using cutadapt (v4.9) [24]. Reads were aligned to the human reference genome (GRCh38) using STAR (v2.7.11d) [25], and transcript-level quantification was performed with Salmon (v1.10.3) [26].

For *YTHDC1*$^{SCON/SCON}$ samples, a custom reference genome and corresponding GTF annotation containing the SCON sequence were used as a reference genome for alignment.

Sashimi plot visualizations were generated using custom Python scripts with the pysam package (v0.22.1) (https://github.com/pysam-developers/pysam). Read coverage on the y-axis was normalized by the effective library size estimated with edgeR and scaled by 1×10^6.

Transcript-level abundances, counts, and transcript lengths were summarized to the gene level using the tximport R package (v1.30.0) [27]. Raw counts were normalized using the trimmed mean of M-values (TMM) method implemented in edgeR (v4.0.16) [28]. Differential gene expression analysis between conditions was evaluated using a negative binomial generalized linear model fitted with glmQLFit, followed by a quasi-likelihood F-test (glmQLFTest). P-values were adjusted for multiple testing using the Benjamini–Hochberg method.

Establishment and maintenance of animal small intestinal organoids

Rhinolophus ferrumequinum small intestinal organoids were kindly provided by the Center for Study of Emerging and Re-emerging Viruses, Korea Virus Research Institute [29]. *Mus musculus* was purchased from Raonbio, and *Rattus norvegicus* was purchased from DBL. Fresh duodenum tissues were harvested from anesthetized *Mus musculus* and *Rattus norvegicus* for organoid generation. All surgical procedures were conducted in accordance with standard protocols approved by the Institutional Animal Care and Use Committee (IACUC) of the Institute for Basic Science [Protocol # IBS-2024–019]. Duodenal tissues were obtained from 18 to 19-day-old *Gallus gallus* embryos, which were sourced from a livestock farm. The embryos were anesthetized, and the duodenum was harvested for organoid generation following IACUC-approved procedures [Protocol # IBS-2025–050]. Duodenum tissue from *Sus scrofa* was purchased from Apures, and duodenum tissue from *Macaca fascicularis* was kindly provided by Professor Jeong Hun Kim at the Fight against Angiogenesis-Related Blindness (FARB) Laboratory, Biomedical Research Institute, Seoul National University Hospital.

Establishment and maintenance of small intestinal organoids

The isolation of small intestinal crypts and the establishment of organoids were performed as previously described [30, 31]. Briefly, isolated small intestines were opened longitudinally and washed with cold 1X PBS. Crypts were isolated using Gentle Cell Dissociation Reagent (Cat# 100–0485, STEMCELL Technologies) at room temperature for 15–30 min. Approximately 40–50 isolated crypts per well were seeded in Matrigel (Cat# 356 231, Corning) and cultured with either human IntestiCult™ Organoid Growth Medium (Cat# 06 010, STEMCELL Technologies) or WENRnic medium (Egf, Noggin, R-spondin1, Wnt surrogate-Fc fusion protein, and nicotinamide). The WENRnic medium was prepared with advanced Dulbeoptionscco's Modified Eagle's Medium (DMEM)/F12 (Cat# 12634–010, Gibco) supplemented with penicillin-streptomycin, 10 mM HEPES (Gibco), GlutaMAX (Gibco), 1X B27 (Cat# 17 504 044, Life Technologies), 10 mM nicotinamide (Cat# N0636, MilliporeSigma), 1.25 mM N-acetyl cysteine (Cat# A9165, Sigma-Aldrich), human Epidermal Growth Factor (hEGF; 50 ng/ml; Cat # AF-100–15, PeproTech), human Noggin (100 ng/ml; Cat# 120–10C, PeproTech), human R-spondin1 (100 ng/ml; Cat# 120–38, PeproTech), Wnt surrogate-Fc fusion protein (0.5 nM), and 10 mM ROCK inhibitor (Tocris). Culture media were changed every 2–3 days. Established organoids were routinely passaged at 1:3 to 1:5 ratios every week and maintained in a culture medium without the ROCK inhibitor.

SCON transfection in the intestinal organoids

The electroporation protocol was adapted from Meranda *et al.* [32]. Organoids of various species were cultured until reaching confluency in at least 24 wells of a 48-well plate to ensure sufficient material for four electroporations (EPs). Five days prior to electroporation, organoids were split at a 1:2 ratio to obtain 24 confluent 48-well plate wells. To optimize electroporation conditions, the culture medium was replaced with EP medium two days before the procedure, followed by an additional medium change to EP medium supplemented with 1.25% DMSO one day prior to electroporation. For electroporation, organoids were dissociated using TrypLE for 5–10 min, followed by gentle pipetting with BSA-soaked tips. The dissociated cells were examined under a microscope to confirm cell clumps containing approximately 10–20 cells. Electroporation was performed using 30 μg of total DNA, consisting of 15 μg of mCherry control plasmid and 15 μg of either an empty vector, GFP vector, eG-SCON-FP, or eG-SC-FP vector. For the 2nd electroporation, 20 μg of the mCherry-IRES-Cre vector was used. Following electroporation, the culture medium was replaced with EP medium containing 1.25% DMSO after 24 h. Imaging was conducted 24 and 72 h after electroporation using the EVOS M7000 microscope. For higher-magnification imaging, organoids were imaged using a 10X objective (NA = 0.45) on a Zeiss LSM 980 confocal microscope.

Quantification and statistical analyses

Statistical analyses were performed using GraphPad Prism10 (GraphPad Software, Inc). Two-way ANOVA with Tukey's

post hoc test was performed for comparisons involving more than two groups of datasets. All analyses were two-tailed, and results were reported as non-significant (ns, $P > 0.05$) or significant ($^{***}P < 0.001$; $^{****}P < 0.0001$).

Illustrations

Schematic illustrations were created with BioRender.com

Establishment of the database for the SCON application

To construct GenPos-SCONDB (https://genpos.org/), we collected genomic information on sequences, exons, coding regions, and gene types that were downloaded from the Ensembl (Release 109) database for a total of 308 species, spanning 91 fish species, 51 bird species, 2 amphibians, 18 reptiles, and 146 mammals, including subspecies and strains (http://www.ensembl.org/) [33]. The front-end interface was developed using Svelte (https://svelte.dev/), while FastAPI (https://fastapi.tiangolo.com/), a high-performance web framework, was employed for back-end data preprocessing and filtering.

To systematically prioritize optimal guide RNAs, candidate sites were evaluated using a comprehensive Combined Score (max.=100). Following the methodology described in previous SCON studies [9] and adapting the scoring criteria of the CHOPCHOP [34], each guide RNA is ranked according to: (i) the mismatch score, which penalizes potential off-target binding (up to 30); (ii) the GC content, favoring an optimal range of 40–70% (up to 30); and (iii) the absence of self-complementarity (up to 10). To advance the previous SCON methodology, we introduced two novel parameters critical for targeted knock-in and knockout efficacy: (iv) distance from cutting site (up to 20), which penalizes the genomic distance between the predicted Cas9 cleavage coordinate and the intended genomic insertion site to maximize integration precision, and (v) the 3N constraint (up to 10), ensuring that any potential cryptic alternative splicing events result in a frameshift and loss of function.

For phylogenetic visualization, we used iTOL [35], a web-based phylogenetic tree visualization tool. The underlying tree data were obtained in the Newick data format from the Ensembl Species Tree section. Canonical transcript mapping was performed using the APPRIS database for selected species, including mice, rats, monkeys, humans, pigs, cows, chickens, and zebrafish (https://appris.bioinfo.cnio.es/#/) [36], where the 'PRINCIPAL:1′ annotation was used to identify the canonical transcript. For all other species, the longest transcript was designated as the canonical transcript. To visualize sequence conservation patterns of introns, sequence logos were generated using WebLogo v3.7.11 [37].

Results

Functional validation of the SCON system targeting the zebrafish *tyr* gene

In our previous study, we demonstrated the versatility of the SCON system across various cell lines using the SCON reporter cassette and mouse endogenous genes [9], and further validated its robustness *in vivo* in mice by targeting 27 endogenous genes (Supplementary Fig. S1 and Supplementary Table S1) [38, 39]. To gain deeper insights into the functionality of the SCON strategy in tractable vertebrate *in vivo* systems, such as zebrafish, we initially designed an SCON-based cKO allele for the *tyrosinase* (*tyr*), based on the GenPos-SCONDB (https://genpos.org/), which encodes an enzyme crucial for converting tyrosine into the pigment melanin [40]. We injected the sgRNA, targeting the first exon of *tyr*, and nuclear-localized Cas9 mRNA [16] with commercially synthesized, 300 bp-long SCON-encoded ssODNs, containing short homology arms (55 bp and 56 bp for the 5′ and 3′ homology arms, respectively) [9] (Supplementary Fig. S2, S3, and Supplementary Table S2), into the one-cell stage of the zebrafish embryos. We quickly verified the knock-in of the SCON cassette at the target locus by analyzing the larval phenotype, which was classified based on pigmentation. Co-injection of the SCON cassette with CRISPR/Cas9 showed increased pigmentation compared to those CRISPR/Cas9-only injections (Supplementary Fig. S3A, B). Furthermore, SCON integration was subsequently verified through genomic PCR and Sanger sequencing (Supplementary Fig. S3C–E). Genotyping and sequencing fin clips from the tyr^{SCON} founders at 2–3 months old led to the identification of three (out of 22) SCON-integrated founder fish: one with precise integration (4.5%) and two with indels (3 bp deletion and 50 bp deletion) (Supplementary Fig. S4). The *tyr* founder with precise integration exhibited a 37.5% germline transmission rate (6 out of 16) in the F1 generation (Supplementary Fig. S4, Supplementary Table S3). To assess the functionality of the SCON system in tyr^{SCON} fish, we generated a homozygous knock-in line through intercrossing of heterozygotes and transiently examined the recombination of loxP by injecting Cre mRNA into the one-cell stage of embryos (Fig. 1A, B). This resulted in the accurate excision of the loxP-flanked region, including the branch point of the $tyr^{SCON/SCON}$ homozygote embryos, leading to a complete loss of pigmentation, compared to embryos that were not injected with Cre mRNA (Fig. 1C, D). These results highlight that the SCON system functions effectively in zebrafish.

Conditional knockout of the zebrafish *sox2* gene enabled by SCON technology

To further examine the functionality of the SCON system for studying lethal genes, we chose to target the *sox2* gene, a developmentally essential gene for swim bladder inflation and motoneuron development [41]. We injected sgRNA targeting the single exon of *sox2*, along with Cas9 mRNA and 300 bp-donor ssODNs into zebrafish embryos (Fig. 2A, B, Supplementary Fig. S5, and Supplementary Table S2). We confirmed the Cas9 endonuclease activity and potential integration of the SCON cassette at the target locus through a brief pooled analysis of larvae in both genotype and phenotypes, characterized by swim bladder inflation failure and minor tail abnormalities (Supplementary Fig. S5). Following fin clipping prescreening, seven out of 106 founder fish were found to have a knock-in after being injected with a 300 bp-long ssODN containing the SCON cassette at the target locus of *sox2*. Among those seven, two had precise integration, while the other five also harbored various indels (Supplementary Fig. S6A). Of the two founder fish with precise integration, only one fish exhibited a 0.92% (1/108) germline transmission rate in the F1 generation (Supplementary Fig. S6B, Supplementary Table S3). In contrast to the *sox2* zebrafish null mutant [41], $sox2^{SCON/SCON}$ homozygous fish are viable and can produce offspring that mature into adulthood (Supplementary Fig. S6C). These results indicate that the SCON cassette does not interfere with the function of *sox2* in the SCON-knock-in zebrafish.

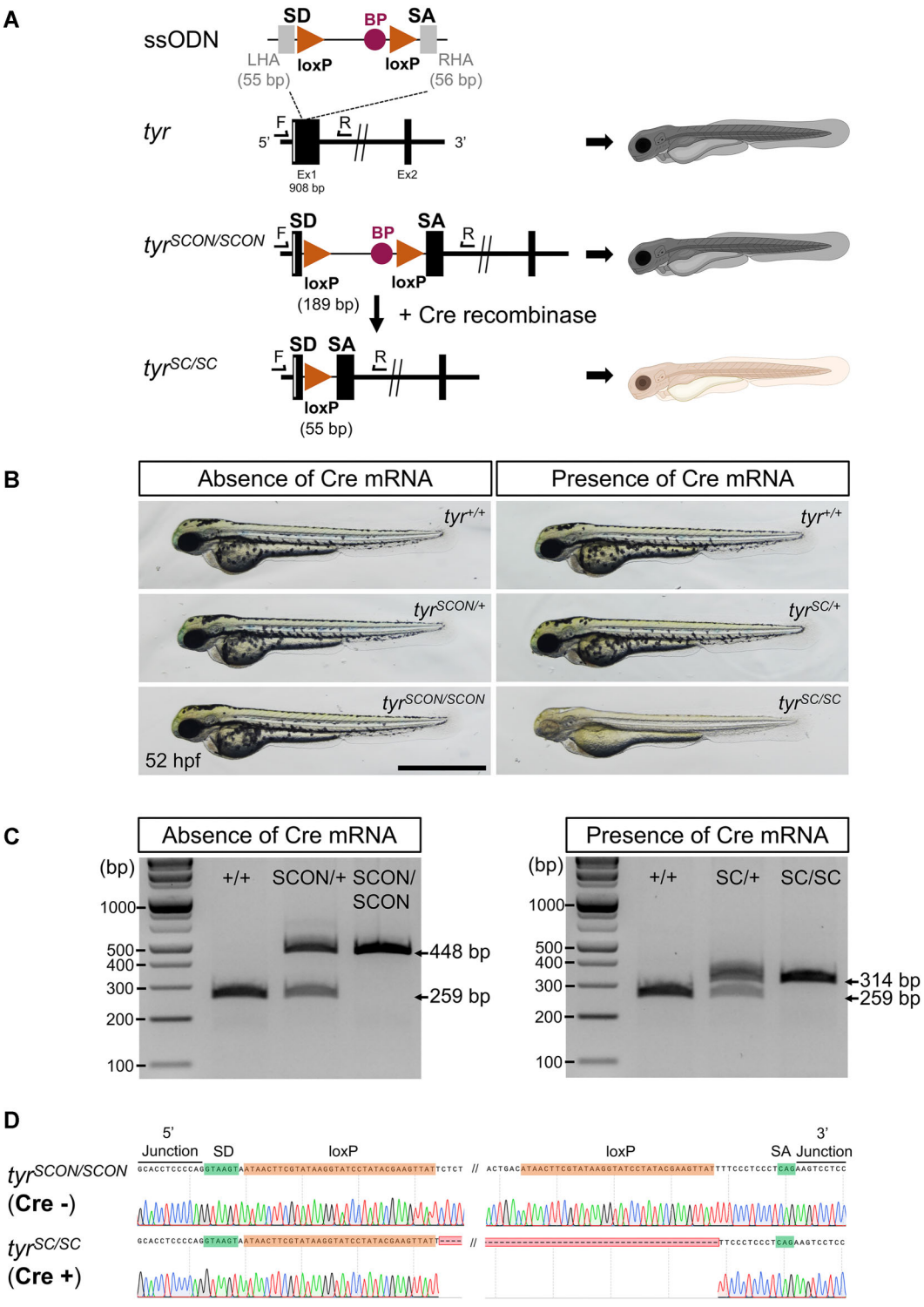

Figure 1. Pigmentation defect of *tyr*$^{SCON/SCON}$ homozygote embryos in the presence of Cre recombinase. (**A**) Schematic illustration of SCON integration at *tyr* locus. BP, branch point; F, forward primer; LHA, left homologous arm; Orange triangles, loxP; R, reverse primer; RHA, right homologous arm; SA, splice acceptor; SC, recombination form of SCON; SD, splice donor; ssODNs, single-stranded oligodeoxynucleotides. Created in BioRender. Kim, S. J. (2026) https://BioRender.com/g1qvviw (**B**) Pigmentation defect in F2 *tyr*$^{SCON/SCON}$ homozygous embryos at 52 hpf following injection of Cre mRNA. Scale bar, 1 mm. (**C**) Genotyping PCR of F2 *tyr*^{SCON} embryos in the absence and presence of Cre recombinase, in which the recombined (314 bp) and non-recombined bands (448 bp). The notations +/+, SCON/+, and SCON/SCON denote wild-type, SCON-heterozygote, and SCON-homozygote, respectively. The notations SC/+ and SC/SC denote the recombination form of SCON-heterozygote, and the recombination form of SCON-homozygote, respectively. (**D**) Sanger sequencing of *tyr*$^{SCON/SCON}$ homozygotes, absence (Cre -) or presence (Cre +) of Cre recombinase, confirmed that the loxP-flanked region was deleted in the presence of Cre recombinase.

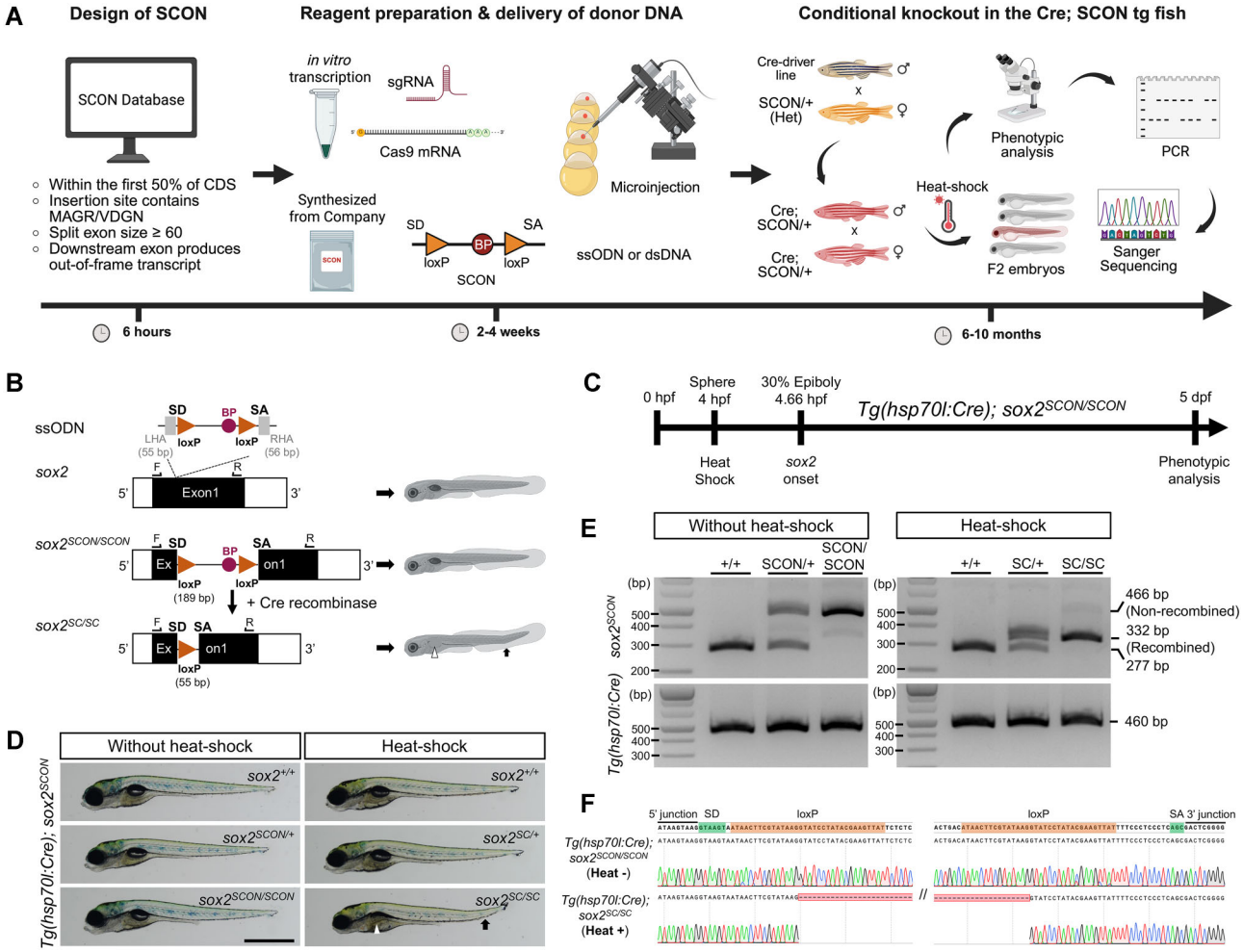

Figure 2. Abnormal development of *sox2*$^{SCON/SCON}$ fish upon heat-induced Cre activation. (**A**) Schematic illustration of the process of a conditional knockout study with SCON knock-in zebrafish. Created in BioRender. Kim, S. J. (2026) https://BioRender.com/hguokv7 (**B**) Schematic illustration of SCON integration at the single exon of *sox2* locus. Created in BioRender. Kim, S. J. (2026) https://BioRender.com/cgeozuk (**C**) Timeline of heat-shock exposure and phenotypic analysis. (**D**) Failure of swim bladder development (white arrowhead) and abnormal tail curvature (black arrow) in *sox2*$^{SCON/SCON}$ homozygous embryos on day 5 following heat exposure. Scale bar, 1 mm. (**E**) Genotyping PCR of F3 *sox2*^{SCON} larvae with or without heat-shock treatment, in which the recombined (332 bp) and non-recombined (466 bp) bands. The notations +/+, SCON/+, and SCON/SCON denote wild-type, SCON-heterozygote, and SCON-homozygote, respectively. The notations SC/+ and SC/SC denote the recombination form of SCON-heterozygote, and the recombination form of SCON-homozygote, respectively. (**F**) Sanger sequencing of *sox2*$^{SCON/SCON}$ homozygotes before and after heat exposure. BP, branch point; dsDNAs, double-stranded DNA; F, forward primer; LHA, left homologous arm; Orange triangles, loxP; R, reverse primer; RHA, right homologous arm; SA, splice acceptor; SC, recombination form of SCON; SD, splice donor; ssODNs, single-stranded oligodeoxynucleotides.

To directly verify the functionality of the SCON system in *sox2* knock-in fish, we induced recombination between the two loxP sites by injecting Cre mRNA. Genomic DNA was then analyzed using PCR genotyping and Sanger sequencing, revealing the removal of the loxP-flanked region in the *sox2*$^{SCON/SCON}$ homozygous knock-in larvae injected with Cre mRNA, compared to those not injected with Cre mRNA (Supplementary Fig. S7A, B). The *sox2*$^{SCON/SCON}$ homozygote larvae that received Cre mRNA showed swim bladder inflation failure and tail curvature, unlike the larvae not exposed to Cre mRNA (Supplementary Fig. S7C).

To perform conditional inactivation of the *sox2* allele *in vivo*, an F2 *sox2*^{SCON} heterozygous fish was crossed with the *Tg (hsp70l:Cre)* line to disrupt the function of *sox2* through the heat-induced Cre recombinase. Since the *sox2* gene expression initiates at the 30% epiboly stage (approximately 4.6 h post-fertilization, hpf) [42], heat shock treatment was administered at 4 hpf in the *Tg (hsp70l:Cre)*; *sox2*^{SCON} larvae to induce controlled gene inactivation (Fig. 2C). The heat-shocked *sox2*$^{SCON/SCON}$ homozygous larvae exhibited failure of swim bladder inflation and mild tail abnormalities compared to those that were not heat-shocked (Fig. 2D). Upon recombination, we confirmed a size shift of the SCON cassette (recombined, 332 bp; non-recombined, 466 bp) via genotyping PCR of *sox2*^{SCON} larvae, indicating the removal of the loxP-flanked region (Fig. 2E, F). These results demonstrate that the SCON enables the conditional knockout of the target gene in zebrafish.

One-step generation of conditional knockout human iPSCs using the SCON system

Next, we applied the SCON strategy to generate cKO alleles in human iPSCs, addressing the challenge of low efficiency in conditional targeting of specific genes in iPSCs [43, 44]. First, we validated the functionality of the SCON system in

human iPSCs using a reporter assay. The iPSCs were transfected with an empty vector, eGFP, eG-SCON-FP, or eG-SC-FP (a recombined form of eG-SCON-FP), together with an mCherry plasmid as a transfection control. These experiments clearly demonstrated the functionality of the SCON system in human iPSCs (Supplementary Fig. S8). To further evaluate the functionality of the SCON cassette in human iPSCs, we generated an eGFP and eG-SCON-FP reporter iPSC line using the PiggyBac transposon system, which maintained the normal expression level of eGFP (Fig. 3A, B, and Supplementary Fig. S9). Three days after independent electroporation of the mCherry-IRES-Cre plasmid into the eGFP and eG-SCON-FP reporter iPSC lines, the PB-eG-SCON-FP line showed mutually exclusive eGFP and mCherry fluorescence, indicating Cre-mediated loss of eGFP expression in the mCherry-positive ($mCherry^+$) population, relative to the eGFP control line (Fig. 3B). Using flow cytometry analysis, we confirmed a substantial reduction in eGFP expression within the $mCherry^+$ population compared to the control, thereby validating the functionality of the SCON system in human iPSCs (Fig. 3C).

Subsequently, we proceeded to test the SCON cassette for targeting endogenous genes. SCON cassette was target integrated into a gene-of-interest in human iPSCs by electroporating Cas9/sgRNA RNP complexes along with the SCON-encoding donor DNA. Following electroporation, individual iPSC clones were isolated through limiting dilution, manually picked, and subsequently expanded for further analysis, all of which takes about 21 days (Supplementary Fig. S9).

To evaluate different forms of SCON templates for cKO in human iPSCs, we tested various types of SCON cassettes, varying in homology arm lengths and strand types (single or double), in seven endogenous genes (Supplementary Table S4). Genomic DNA PCR confirmation showed an average targeting efficiency of 16.0 ± 8.8% (mean ± SD) for SCON integration (Supplementary Table S4). Synthesized double-strand SCON templates with longer homology arms (500 bp to 1 kb) showed comparable integration efficiency (15.3 ± 9.7%, mean ± SD), making it a relatively cheap option with good efficiency. With higher single allele targeting efficiency, these results indicate that bi-allelic SCON integration (4.3 ± 2.4%, mean ± SD) is feasible for one-step generation of cKO human iPSCs without the need for selection processes using fluorescent or drug-resistant cassettes (Supplementary Fig. S1B).

Efficient SCON-mediated conditional knockout of developmentally essential genes in human iPSCs

To confirm our strategy functions well for endogenous genes, we selected two essential genes, *YTHDC1* (Fig. 4) and *CTNNB1* (Supplementary Fig. S10), as the SCON targets based on the GenPos-SCON database, both of which are involved in embryonic development. *YTHDC1* encodes a key nuclear m^6A reader protein that regulates RNA splicing, nuclear export, and stability, which are critical processes for gene expression [45]. During development, *YTHDC1* is crucial for properly maintaining embryonic stem cells and plays a major role in early embryogenesis [46]. We targeted exon 3 of the *YTHDC1* gene and generated the $YTHDC1^{SCON/SCON}$ (homozygote) iPSCs line (Fig. 4A, B). To verify whether $YTHDC1^{SCON/SCON}$ iPSCs are conditionally regulated, we used the lentivirus expressing CreERT2 under the *EF1α* promoter to induce Cre-mediated recombination. Following the lentiviral infection of $YTHDC1^{SCON/SCON}$ iPSCs, cells were treated with 4-hydroxytamoxifen (4-OHT) to induce Cre-mediated recombination. We confirmed the recombination using PCR genotyping at 12, 24, and 48 h following 4-OHT treatment. Nearly all cells showed recombination after 48 h of 4-OHT treatment, compared to untreated cells, through PCR genotyping and Sanger sequencing, with the expected PCR amplicon sizes being 660 bp for WT (wild-type), 849 bp for SCON (non-recombined SCON allele), and 715 bp for SC (recombined SCON allele) (Fig. 4C, D). To further characterize the $YTHDC1^{SCON/SCON}$ knock-in line at the transcriptional level, we performed bulk RNA sequencing of wild-type and $YTHDC1^{SCON/SCON}$ homozygous knock-in iPSCs, with and without 4-OHT treatment. Although a minor fraction of transcripts (~4%) showed aberrant splicing at the introduced junction (Supplementary Fig. S11A, B), 4-OHT-induced recombination produced a clear, time-dependent decrease in YTHDC1 expression (Supplementary Fig. S11C).

To verify the conditional knockout of YTHDC1 expression, we performed immunofluorescence labeling on CreERT2-lentivirus-infected $YTHDC1^{+/+}$ (WT) and $YTHDC1^{SCON/SCON}$ (homozygote) iPSCs with and without 4-OHT treatment. In the absence of 4-OHT, the YTHDC1 protein was clearly detectable, predominantly in the nucleus. However, in $YTHDC1^{SCON/SCON}$ (homozygote) iPSCs treated with 4-OHT, YTHDC1 expression was absent, confirming a successful conditional knockout through the SCON system (Fig. 4E). Due to the essential role of *YTHDC1*, $YTHDC1^{SCON/SCON}$ iPSCs begin to die 48 h following 4-OHT treatment. To verify this, we conducted cleaved Caspase-3 staining to assess the cell death at 72 h (Fig. 4F, G) and performed an MTT assay to measure cytotoxicity levels for four days, both revealing an increase in cell death after 4-OHT treatment (Fig. 4H).

To further validate the functionality of the SCON system, we targeted the exon 5 of the *CTNNB1* gene (Supplementary Fig. S10A), which encodes *β-catenin*, a key component of the Wnt signaling pathway involved in maintaining cellular homeostasis [47]. Functional $CTNNB1^{SCON/SCON}$ homozygous iPSCs were verified by PCR genotyping at 12, 24, and 48 h after 4-OHT treatment. PCR genotyping and Sanger sequencing showed that nearly complete recombination occurred after 48 h of treatment compared with untreated cells (Supplementary Fig. S10B, C). Immunofluorescence images showed slightly decreased levels of CTNNB1 protein expression before 4-OHT treatment, although the $CTNNB1^{SCON/SCON}$ homozygous knock-in line exhibited a tolerable degree of hypomorphic effect relative to WT controls (Supplementary Fig. S10D). Notably, efficient conditional knockout of the *CTNNB1* gene was clearly observed after 48 h of 4-OHT treatment (Supplementary Fig. S10D). Together, these findings demonstrated that the SCON system enables conditional knockout of developmentally essential genes in human iPSCs.

Conserved functionality of SCON across vertebrate species

In our earlier work, we demonstrated the effectiveness of SCON as a potential conditional knockout tool in zebrafish (*Danio rerio*), frogs (*Xenopus laevis*), and four mammalian cell lines using SCON reporter cassettes, and further targeted an endogenous mouse locus with a SCON cassette [9]. In the present study, we extended these findings by validating

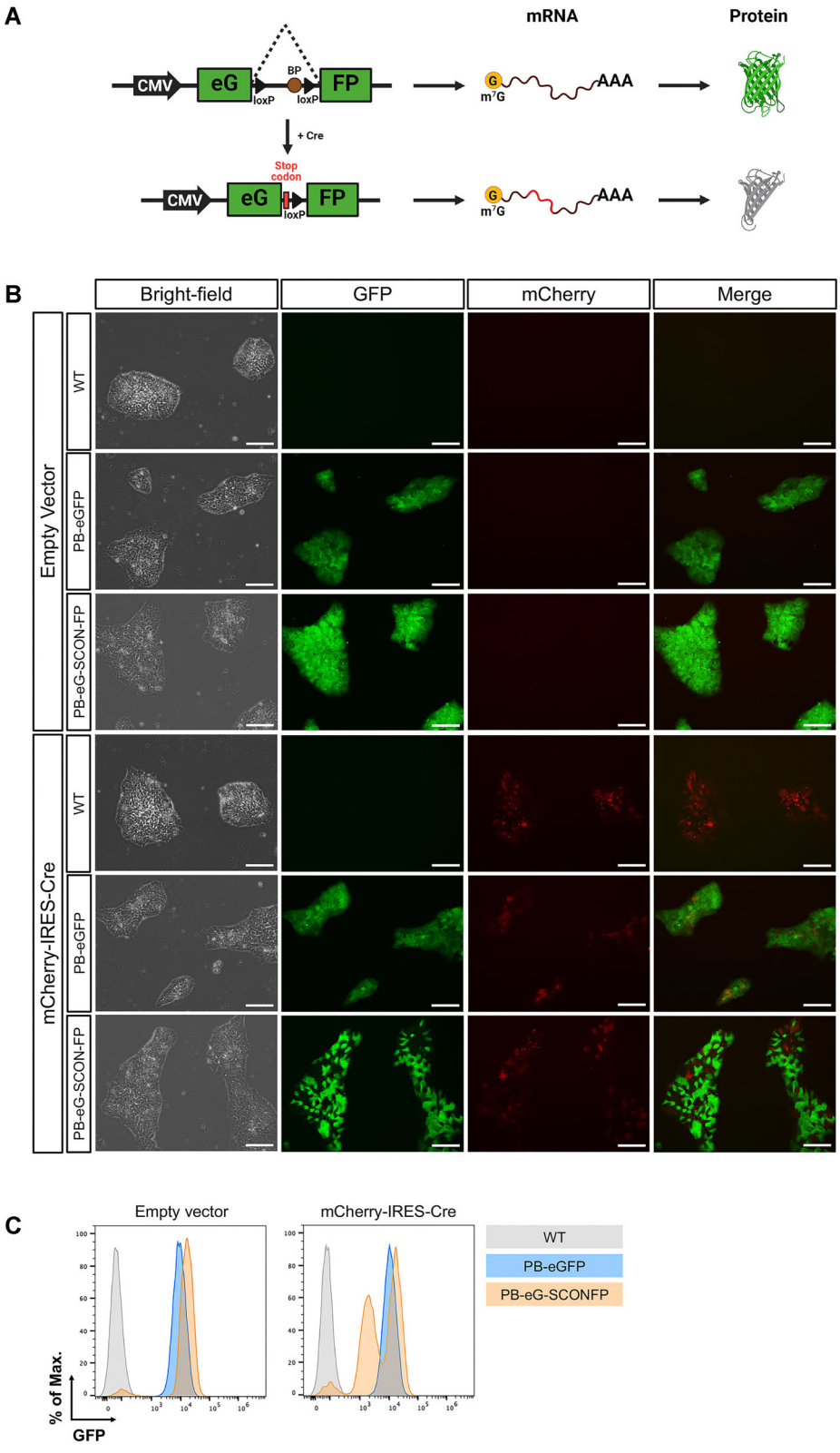

Figure 3. Validation of the SCON system with eG-SCON-FP iPSCs. (**A**) A schematic representation of the SCON functionality test in an eGFP construct, showing the eG-SCON-FP and the recombinant eG-SC-FP forms. Created in BioRender. Kim, S. J. (2026) https://BioRender.com/1b4nma9 (**B**) Fluorescence microscopy images of WT, PB-eGFP, and PB-eG-SCON-FP iPSCs following electroporation with either an empty vector or the mCherry-IRES-Cre plasmid show a reduction in eGFP fluorescence within the mCherry^{+} population. This decrease indicates successful excision of the loxP-flanked sequence and demonstrates Cre-mediated conditional suppression of eGFP expression. Scale bar, 100 μm. (**C**) A histogram illustrating the flow cytometry analysis of WT (grey), PB-eGFP (blue), and PB-eG-SCON-FP (orange) iPSCs transfected with either an empty vector or mCherry-IRES-Cre vector. Compared to the empty vector control (left), flow cytometry analysis three days post-electroporation shows a marked decrease in eGFP expression in the mCherry-IRES-Cre-transfected group (right), specifically in the PB-eG-SCON-FP iPSC population, supporting the functional activity of the SCON system.

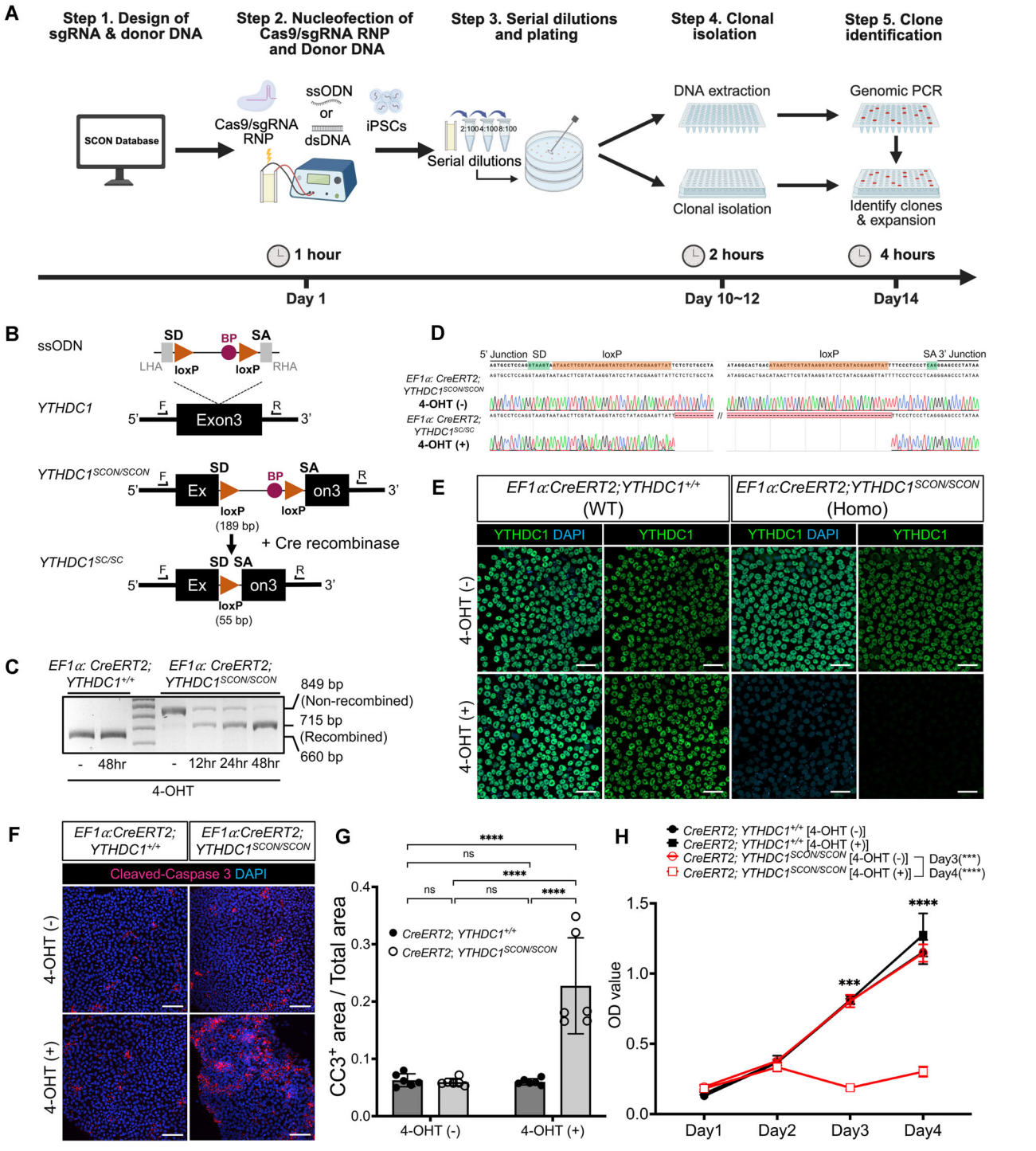

Figure 4. Conditional knockout of *YTHDC1*^{SCON} in knock-in human iPSCs induced by Cre recombinase. (**A**) A schematic illustration of the process of conditional knockout in iPSCs. Created in BioRender. Kim, S. J. (2026) https://BioRender.com/cwi6q2f (**B**) Schematic illustrations depict the integration of the SCON cassette into the exon 3 of the *YTHDC1* locus using ssODN. Primers labeled as F and R were used, with PCR amplicon sizes noted as follows: WT (660 bp), SCON (849 bp), and SC (715 bp). BP, branch point; SA, splice acceptor; SC, recombination form of SCON; SD, splice donor. (**C**) Genotyping PCR analysis of WT and *YTHDC1*$^{SCON/SCON}$ at various time points (0, 12, 24, and 48 h) post-treatment with 4-OHT after infection with *EF1α:CreERT2* lentivirus. (**D**) Sanger sequencing results show the 5′ and 3′ junctions for the homozygous knock-in of *YTHDC1*. Cre-mediated recombination removes the sequences between loxP sites, resulting in a premature stop codon and creating a non-functional protein. (**E**, **F**) Immunocytochemistry of CreERT2; WT and CreERT2; *YTHDC1*$^{SCON/SCON}$ was performed after treatment with either 4-OHT or vehicle, showing YTHDC1 in green and DAPI staining in blue at 48 h (e, scale bar: 50 μm), and cleaved-Caspase 3 (CC3) in red with DAPI staining in blue at 72 h (f, scale bar: 100 μm). (**G**) Quantification of CC3-positive (CC3^{+}) cells in Figure f was analyzed using a Two-way ANOVA, which revealed a significant effect of each group [$F_{(1, 20)} = 22.44$, $P = 0.0001$], 4-OHT treatment [$F_{(1, 20)} = 22.72$, $P = 0.0001$], and interaction [$F_{(1, 20)} = 24.26$, $P < 0.0001$]. Post-hoc analysis was conducted using Tukey's multiple comparisons. The data represent $n = 6$ independent images. (**H**). Cell growth curves of CreERT2; WT and CreERT2; *YTHDC1*$^{SCON/SCON}$, with or without 4-OHT treatment, were assessed using the MTT assay. Two-way ANOVA reveals a significant effect of each group [$F_{(1.042, 3.127)} = 238.4$, $P = 0.0005$], time [$F_{(1.023, 3.070)} = 615.0$, $P = 0.0001$], and interaction [$F_{(1.678, 5.035)} = 84.50$, $P = 0.0002$]. Post-hoc analysis was conducted using Tukey's multiple comparisons. Data represent $n = 4$ independent experiments. For g-h, data are presented as mean ± SD.

SCON in endogenous genes of zebrafish and human iPSCs. To further broaden SCON application to a wider variety of species, we used intestinal organoids derived from six different species, including mouse (*Mus musculus*), rat (*Rattus norvegicus*), chick (*Gallus gallus*), bat (*Rhinolophus ferrumequinum*), pig (*Sus scrofa*), and monkey (*Macaca fascicularis*), transfecting them with an empty vector, eGFP, eG-SCON-FP, or eG-SC-FP (A recombined version of eG-SCON-FP) along with an mCherry plasmid for transfection control. All tested species showed clear functionality of the SCON system as a universal tool for conditional knockout approaches (Fig. 5A, B, and Supplementary Fig. S12A). To confirm our strategy functions well in organoids, stable eGFP and eG-SCON-FP expressing rat small intestinal organoids were generated with the PiggyBac system to assess the SCON functionality in 3D *in vitro* systems (Fig. 6A, Supplementary Fig. S12B, and S13). After electroporation of the mCherry-IRES-Cre plasmid, a retention of GFP can be seen in GFP organoids, while eG-SCON-FP rat organoids lost their GFP expression (Fig. 6B, Supplementary Fig. S12B, and S13). These results highlight that SCON works as expected within organoid systems.

GenPos-SCONDB: Precalculated database for SCON design

The generation of SCON-based transgenic models requires several considerations, including SCON target sites, sgRNA design, and ssODN with homologous arms. To facilitate this, the user-friendly GenPos-SCONDB website (https://genpos.org/) provides pre-calculated essential information to facilitate SCON applications across over 300 vertebrate species (Fig. 7A). We developed a custom computational approach based on the selection criteria [9, 48] to identify potential SCON targetable sites across multiple species genomes, incorporating all transcript isoforms to ensure comprehensive coverage. SCON targetability was defined using three strict exon selection criteria. First, target exons must reside within the initial 50% of the protein-coding sequence. Second, they must contain an intron insertion site matching either the MAGR [(A/C)-A-G- (A/G)] or VDGN [(A/G/C)- (A/T/G)-G-(A/T/G/C)] splice junction consensus sequences. Finally, target exons must exceed 120 bp in total length, specifically ensuring that the SCON insertion splits the exon into 5′ and 3′ segments that are each greater than 60 bp. (Supplementary Fig. S14). Despite these stringent criteria, an average of 76.79% of protein-coding genes across the nine species analyzed had targetable MAGR insertion sites, while an average of 86.09% contained targetable VDGN insertion sites (Fig. 7A). The scope of targetable genes can be extended by using Cas9 with a broader PAM sequence, such as xCas9 and SpCas9-NG [49]. It is also possible to utilize the SCON strategy in an untargetable site by generating the required intron insertion site through silent mutations (Supplementary Table S7).

To evaluate the compatibility of the SCON sequence with intronic sequences for diverse species, we identified consensus intron sequences across all species in our database. Our analysis revealed that the SCON sequence closely aligns with conserved splice donor (SD) and splice acceptor (SA) sequences, along with significant similarity in the polypyrimidine tract (Fig. 7B). Interestingly, *Drosophila melanogaster* displays a consensus sequence distinct from other species, while *C. elegans* exhibits a unique consensus sequence, especially within the polypyrimidine tract (Fig. 7B).

In some cases, cryptic alternative splicing may lead to in-frame events interfering with the outcome of SCON-based cKOs (Supplementary Fig. S15, S16). However, it is possible to minimize the risk by designing the undesired alternative splicing to produce a transcript with out-of-frame, meaning that the split 5′ segment of the target exon is out-of-frame with the coding frame of the subsequent exon [8, 12] (Fig. 7C, Supplementary Fig. S17). Notably, out-of-frame events account for 91.5% of SCON-targetable genes at MAGR insertion sites and 99.2% at VDGN insertion sites (Fig. 7C).

The GenPos-SCONDB website (https://genpos.org/) provides SCON targetable sites and sources for designing sgRNA, such as target and PAM sequences, GC contents, self-stem scores, mismatch scores, the 3N constraint, the distance from cut, and the comprehensive combined score. Users can download all of this information, along with the corresponding ssODN sequences for each target site. The result page shows detailed information about transcripts and exons and visualization of sequences and target regions with highlights for PAM sequences and SCON insertion sites (Fig. 7D).

Discussion

The SCON system, with a combination of CRISPR/Cas9 and HDR, enables the generation of model animals for conditional knockout through cassette insertion at the targeted genomic region based on the suggested targets from the GenPos-SCONDB (https://genpos.org/). We achieved precise site-specific insertions of the SCON cassette at endogenous loci in both zebrafish and human iPSCs, leading to the generation of stable knock-in transgenic lines. Moreover, we validated the functional activity of the SCON construct across diverse intestinal organoids derived from multiple species, highlighting its broad applicability across biological systems. To facilitate broader adoption and optimize experimental design, we developed a user-friendly web-based platform, GenPos-SCONDB (https://genpos.org/). This platform enables researchers to predict optimal SCON insertion sites within genes of interest and to design corresponding donor DNA constructs. Collectively, these results highlight the potential of the SCON system as a powerful and adaptable tool for precise genome engineering and functional studies in both *in vivo* and *in vitro* models.

The SCON system represents an advancement designed to circumvent the challenges presented by earlier conditional mutagenesis methodologies in zebrafish. Gene-trap-based methods, such as Zwich [50] and Uflip [51], were developed for conditional mutagenesis. These approaches rely on the integration of a gene trap cassette, frequently containing a reporter gene, into an intron of the target gene. While the reporter gene's expression, driven by the endogenous promoter, facilitates efficient screening of mutant fish, a notable limitation is the requirement for large and complex donor vectors, which are often challenging and time-consuming to design and construct. The Cre-controlled CRISPR (3C) mutagenesis system, conversely, utilizes Tol2-mediated transgenesis, which can result in the random insertion of multiple transgene copies into the genome [52]. Such random integration can lead to variable expression levels and potential off-target effects attributable to position effects. In contrast, the SCON technology directly targets exons, rendering it applicable to all transcripts derived from the target gene and enabling its utility

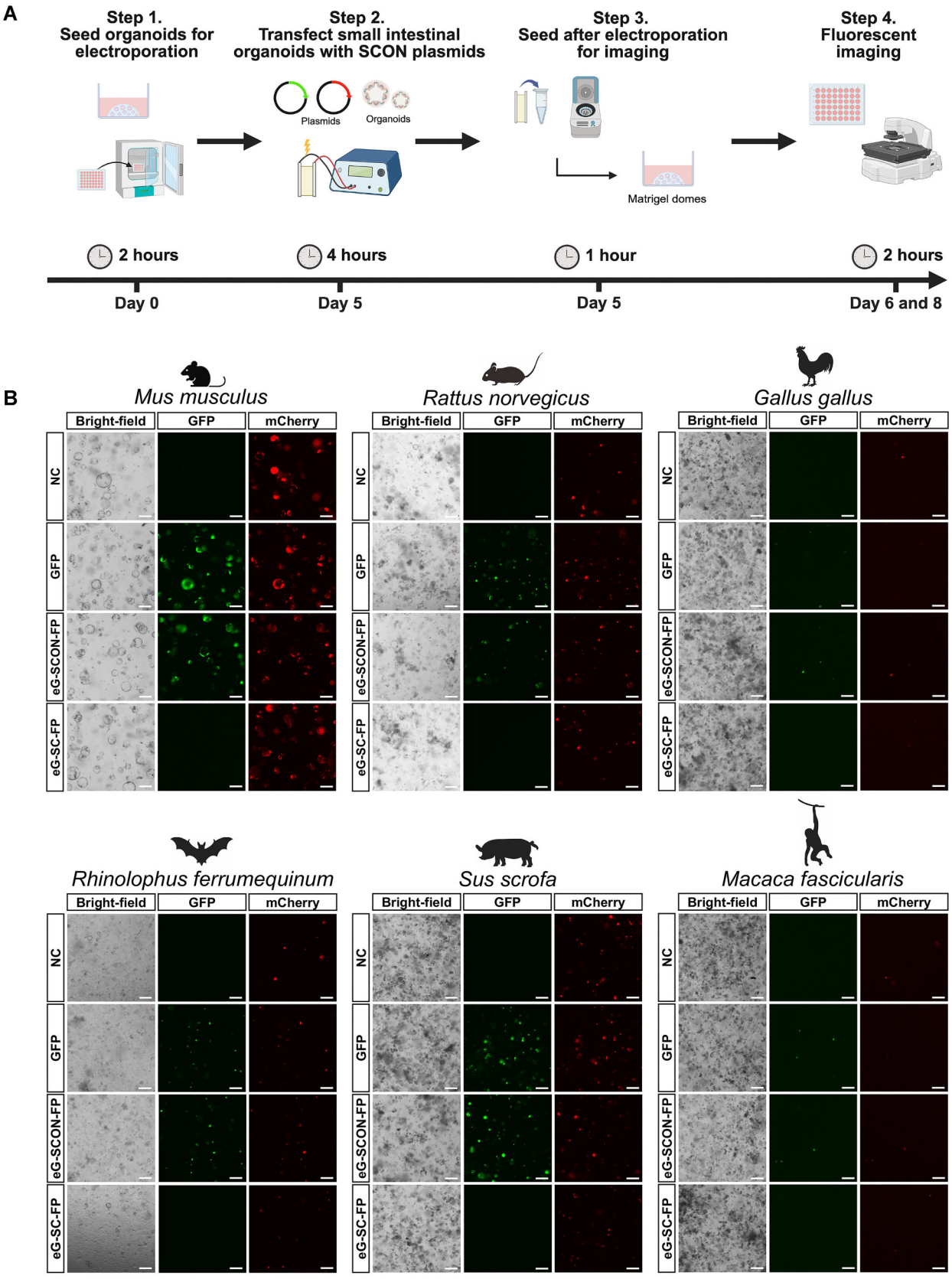

Figure 5. Expand the SCON application in the small intestinal organoids from various species. (**A**) A schematic illustration of the overexpression experiment process in small intestinal organoids using electroporation. Created in BioRender. Kim, S. J. (2026) https://BioRender.com/pq2rmf3 (**B**) Representative intestinal organoid images of empty vector (NC, negative control), GFP, eG-SCON-FP, or eG-SC-FP electroporated organoids in mouse (*Mus musculus*), rat (*Rattus norvegicus*), chick (*Gallus gallus*), bat (*Rhinolophus ferrumequinum*), pig (*Sus scrofa*), and monkey (*Macaca fascicularis*). Images were taken 3 days after electroporation, where the monkey and chick used 5x the GFP intensity that was used for the images. Scale bar, 200 μm. Created in BioRender. Kim, S. J. (2026) https://BioRender.com/q9k56sn.

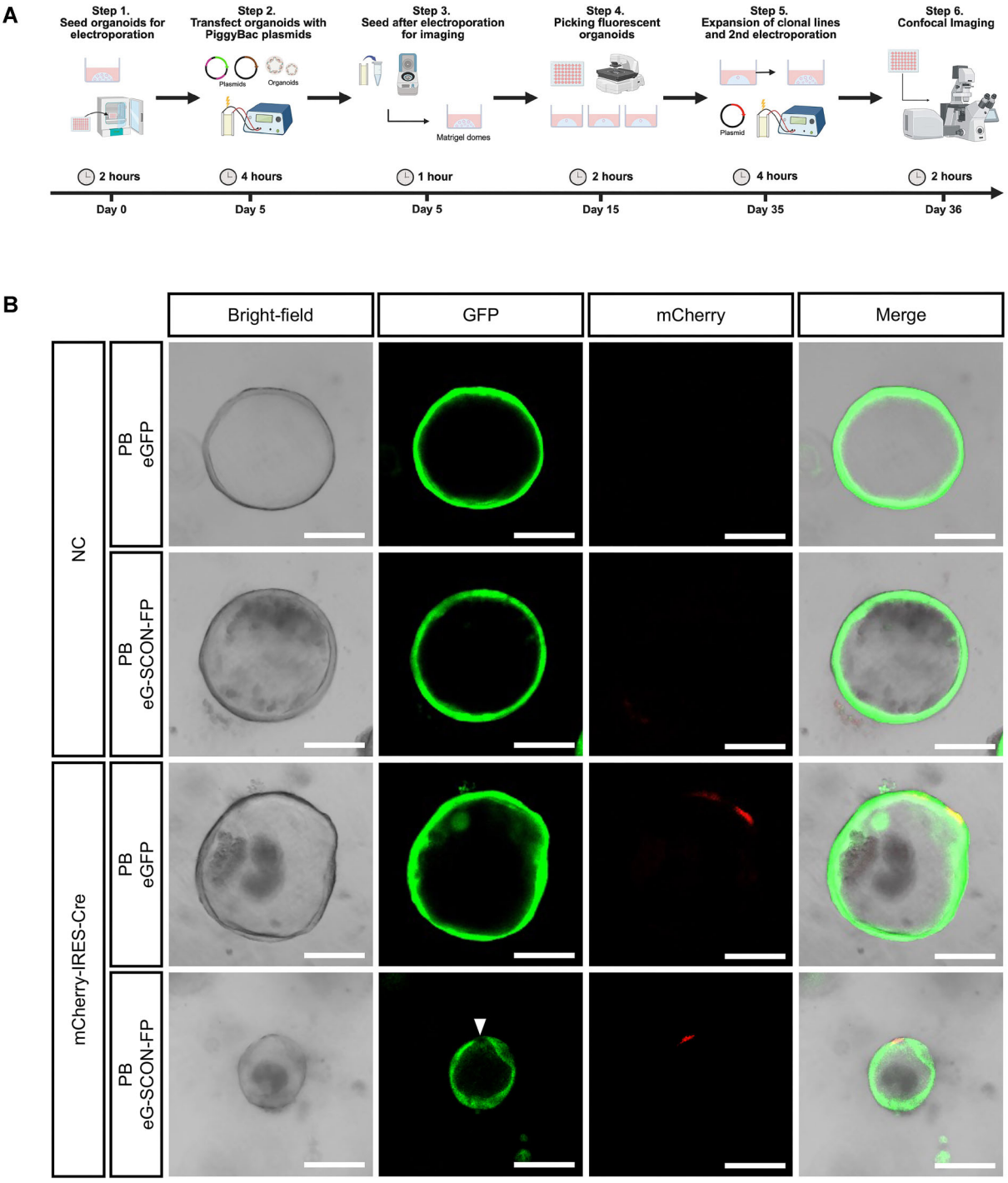

Figure 6. Recombination of the SCON cassette in the rat small intestinal organoids. (**A**) Experimental scheme for testing Cre-mediated recombination of a G-SCON-FP cassette in organoids. Created in BioRender. Kim, S. J. (2026) https://BioRender.com/d4skeux (**B**) Representative images of rat (*Rattus norvegicus*) small intestinal organoids electroporated with PiggyBac eGFP or PiggyBac eG-SCON-FP constructs, following transfection with the mCherry-IRES-Cre plasmid, demonstrate reduced eGFP fluorescence (arrowhead) in the mCherry-positive (mCherry^{+}) population. PB, PiggyBac. Scale bar, 100 μm.

for conditional knockout of most genes, including transcript isoforms and single-exon genes.

Despite these significant advancements, the efficiency of germline transmission in certain model organisms, such as zebrafish, presents unique challenges. The efficiency of germline transmission in zebrafish exhibits locus-specific variability, as evinced by the differential outcomes observed in *tyr* and *sox2* SCON knock-in transgenic lines. This variability may be partially attributed to the restricted temporal window available for DNA delivery during early embryogenesis. While HDR-mediated genome editing has been successfully implemented in zebrafish, it remains technically more challenging than in mammalian systems, such as mice. A contributing factor is the rapid rate of embryonic cell divisions in zebrafish, with post-fertilization cell cycles occurring in less than 1 h, contrasting with the 16–20 h cycles observed in mice; this severely

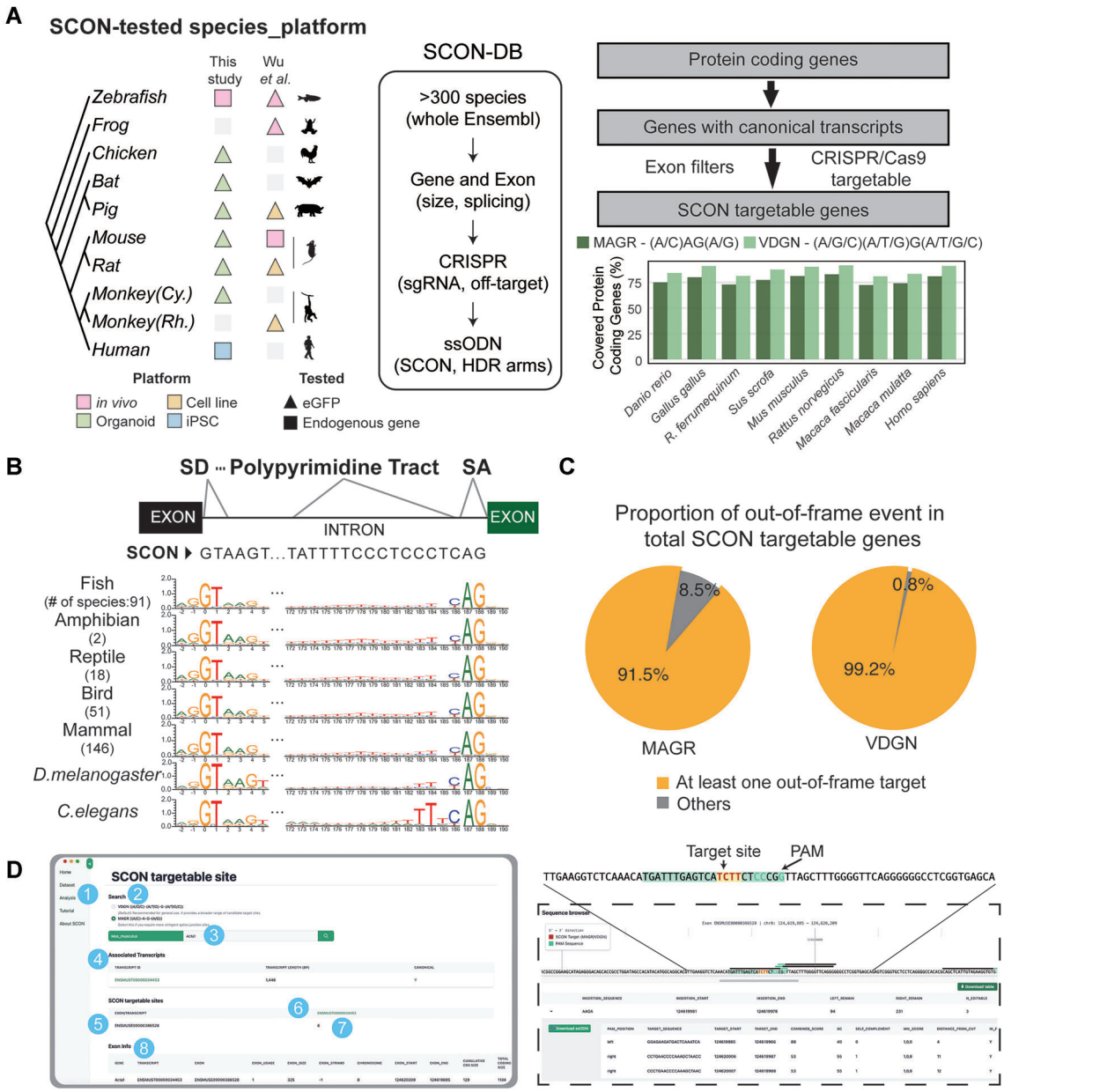

Figure 7. Comprehensive analysis of SCON targetable sites across species and development of the SCON-DB web application. (**A**) A phylogenetic tree and SCON-applied model are shown for ten species: Zebrafish (*Danio rerio*), Frog (*Xenopus laevis*), Chicken (*Gallus gallus*), Bat (*Rhinolophus ferrumequinum*), Pig (*Sus scrofa*), Mouse (*Mus musculus*), Rat (*Rattus norvegicus*), and two Monkey species (Cy., *Macaca fascicularis*; Rh., *Macaca mulatta*), as well as Human (*Homo sapiens*). SCON-DB provides data on SCON targetable sites across 308 species, including these ten. Colored boxes indicate the platforms (such as *in vivo*, cell lines, organoids, and iPSCs) used in each study, while light-gray shapes represent platforms that were not investigated in the corresponding paper. An eGFP construct (black triangle) and endogenous genes (black square) are tested. Gene coverage of exon filters and CRISPR/Cas9 target sites in nine species. The silhouette image of *Xenopus laevis* was obtained from PhyloPic (http://phylopic.org), created by Ian Quigley, and used under the Creative Commons Attribution 3.0 license. (**B**) Weblogo comparison of SCON sequences and consensus intron sequences across different species classes, with the size of each base indicating its bit score. (**C**) Proportion of out-of-frame events in total SCON targetable genes. (**D**) The GenPos-SCONDB (https://genpos.org/) provides a step-by-step process for identifying and analyzing SCON-targetable sites. To use this feature, 1, Select either MAGR or VDGN; 2, Choose the species of interest; 3, Enter the gene where you intend to insert the SCON cassette. 4, Check the list of transcripts associated with the inserted gene; 5 and 6, Check the exon ID and transcript ID to ensure accuracy; 7, Check the number of SCON-targetable sites present in the exon and transcript, and access detailed information about the selected exon; 8, The sequence browser, displayed on the right panel, offers a detailed description of each SCON-targetable site. By clicking on a target sequence, the corresponding top exon sequence is highlighted. Key features include the red sequence representing the target site (MAGR or VDGN), the green sequence indicating the PAM position, and the green highlight marking the target sequence.

constrains the window for effective homology-directed repair [53]. To mitigate these limitations, several small molecules, including SCR7, RS-1, and NU7441, have been utilized to enhance HDR efficiency in zebrafish embryos [53–55].

Beyond its precise targeting capabilities, the SCON system offers distinct advantages over existing methods. Compared to the DECAI [6] and the AIv4 [7, 8, 12] cassette systems, the SCON technology is generally favored due to its enhanced efficiency in generating out-of-frame splice variants following branchpoint removal. This process enhances nonsense-mediated decay (NMD), thereby improving the efficiency of gene disruption [11]. An additional advantage of SCON is its compatibility with both Cre and Flp recombinase systems, as the loxP site can be easily substituted with an FRT site [9, 10]. This expands its utility across a wider range of species, including fish, frogs, birds, mice, rats, bats, pigs, and non-human primates. In widely used animal models like zebrafish and mice, functional gene knockouts are typically achieved through breeding strategies that produce homozygous offspring from heterozygous founders. In contrast, generating bi-allelic modifications in iPSCs presents significant challenges. Due to a low editing efficiency, this often requires extensive screening of numerous clones or the implementation of multiple sequential rounds of genome editing. These efforts are further complicated by the slow proliferation, clonal variability, and sensitivity of iPSCs to genetic manipulation, making the careful optimization of editing conditions and clonal selection protocols essential for success [6, 43, 44]. To address these limitations, the SCON technique provides a practical and efficient approach for generating bi-allelically modified clones without relying on drug selection or fluorescent markers, leading to a more straightforward and effective approach for generating modified iPSCs.

Despite its several advantages, the SCON cassette has a limitation: the potential induction of alternative splicing events following cassette integration. Consistent with our observations, a recent study by Koirala *et al.* (2025) [12] reported that improper placement of artificial intron cassettes within the target exon can result in aberrant splicing and diminished or abolished basal gene expression prior to Cre-mediated recombination. This finding suggests that such effects represent an inherent challenge of artificial intron–based conditional systems rather than a limitation specific to the SCON cassette.

In our previous study, no aberrant splicing was detected at the *Ctnnb1* and *Sox2* loci in mice [9]. Nevertheless, as reported in the AIv4 system (an alternative version of the DECAI cassette) [7, 8] in mice, integration of the SCON cassettes may result in a partial hypomorphic effect. When the SCON cassette was applied to endogenous loci in zebrafish and human iPSCs, unintended cryptic alternative splicing events were observed. To mitigate this limitation, the SCON cassette should be strategically inserted out-of-frame with respect to the downstream exon to induce a frameshift. Although frameshifted transcripts may be partially eliminated by nonsense-mediated mRNA decay, conditional mutants of essential genes generated using the SCON system generally retain sufficient loss of function to support meaningful gene function analyses, while offering advantages over conventional knockout approaches.

Ultimately, the successful application of the SCON strategy is contingent upon the meticulous design and precise delivery of donor DNA to the target locus. A critical factor influencing the efficiency of SCON-mediated knock-in is the selection of an appropriate target site and the design of donor DNA that facilitates accurate integration. Given that the SCON system disrupts gene function by introducing a premature stop codon, we prioritized SCON insertions within the first 50% of the coding sequence, thereby increasing the probability of disrupting essential protein functions. However, the functional outcomes of targeting specific regions within a gene or protein are not yet fully predictable. Addressing this limitation will necessitate the development of computational tools capable of assessing the functional significance of individual protein domains and informing optimal insertion site selection. Such advances would enhance both the efficiency and precision of SCON-mediated genome editing and expand its utility across a broader range of genes, cell types, and experimental contexts. Importantly, the utility of our database extends beyond the SCON system; it is broadly applicable to any genetic engineering model that requires the exon-targeted insertion of artificial introns. To ensure long-term relevance, we plan to continuously synchronize GenPos-SCONDB with the latest Ensembl database release. Furthermore, future updates will expand our repertoire to support other CRISPR effector nucleases that recognize diverse PAM sequences, broadening the targeting scope beyond the currently implemented SpCas9 system.

Taken together, we presented a straightforward, universal tool for conditionally knocking out specific genes across different species, demonstrating that human-derived Short Conditional intrON (SCON) is effective in a wide range of organisms. Additionally, using 'GenPos-SCONDB' (https://genpos.org/) for experimental design will promote broader and more accessible adoption of the system, paving the way for its application in a wider range of animal models, including non-human primates and mini-pigs.

Acknowledgements

We thank the Core facilities and Transgenic team at the Center for Genome Engineering at the Institute for Basic Science (IBS) for their support in maintaining the mouse and fish facilities, and the Virus facility at the IBS for kindly providing the LV-CreERT2-2A-GFP vector and lentivirus. We also thank the Research Solution Center (RSC) of the IBS for performing the flow cytometry analysis. Zebrafish AB line was provided by the Zebrafish Center for Disease Modeling (ZCDM), Republic of Korea. The graphical abstract was created in BioRender. Kim, S. J. (2026) https://BioRender.com/8m9rz8g.

Author contributions: J.-H.C. (Investigation [equal], Methodology [equal], Resources [equal], Validation [equal], Writing – original draft [lead], Writing – review & editing [lead]), J.M. (Investigation [equal], Methodology [equal], Resources [equal], Writing – original draft [equal], Writing – review & editing [equal]), Y.O. (Investigation [equal], Methodology [equal], Software [equal], Writing – original draft [equal], Writing – review & editing [equal]), T.M.K. (Investigation [equal], Methodology [equal], Writing – review & editing [supporting]), Y.K. (Investigation [supporting], Methodology [supporting], Resources [equal]), G.B. (Investigation [supporting], Methodology [supporting], Resources [equal]), Y.K. (Software [supporting]), Yeongjun Kim (Investigation [supporting], Methodology [supporting]), S.L. (Investigation [supporting], Methodology [supporting]), S.P. (Resources [supporting]), J.H. (Resources [supporting]), O.K. (Software [supporting]), Y.K.C. (Resources [supporting]),

J.H.K. (Resources [supporting]), J.-H.L. (Validation [supporting]), J.P. (Software [supporting], Supervision [supporting]), J.K.K. (Software [supporting], Supervision [supporting]), D.H.W. (Funding acquisition [supporting], Supervision [supporting]), K.-J.Y. (Supervision [equal], Writing – review & editing [supporting]), B.-K.K. (Conceptualization [lead], Methodology [supporting], Resources [supporting], Supervision [lead], Writing – review & editing [lead]), H.L. (Conceptualization [equal], Software [lead], Supervision [equal], Writing – review & editing [equal]).

Supplementary data

Supplementary data is available at NAR online.

Conflict of interest

None declared.

Funding

National Research Foundation of Korea (NRF) (2020M3A9E403967022, RS-2024-00440778); National Research Council of Science & Technology (NST) grant by the Korea government (MSIT) (GTL24022-000); Institute for Basic Science (IBS-R021-D1). Funding to pay the Open Access publication charges for this article was provided by the Institute for Basic Science.

Data availability

The bulk RNA-seq data that support the findings of this study have been deposited in the NCBI Sequence Read Archive (SRA) under the BioProject accessions provided in PRJNA1435743.

The source code underlying this study is available on https://github.com/bis-lab/scondb and https://doi.org/10.5281/zenodo.19735707. For any queried gene, the list of SCON targetable sites and corresponding ssODN sequences can be downloaded from the 'Analysis' section of our web database (https://genpos.org/analysis). To access the full dataset, the result files have been deposited in Figshare (https://doi.org/10.6084/m9.figshare.30171820).

References

1. Skarnes WC, Rosen B, West AP. *et al.* A conditional knockout resource for the genome-wide study of mouse gene function. *Nature* 2011;474:337–42. https://doi.org/10.1038/nature10163
2. Kang Y, Chu C, Wang F. *et al.* CRISPR/Cas9-mediated genome editing in nonhuman primates. *Dis Model Mech* 2019;12:dmm039982. https://doi.org/10.1242/dmm.039982
3. Kalvaitytė M, Balciunas D. Conditional mutagenesis strategies in zebrafish. *Trends Genet* 2022;38:856–68. https://doi.org/10.1016/j.tig.2022.04.007
4. Chen Y, Cao J, Xiong M *et al.* Engineering human stem cell lines with inducible gene knockout using CRISPR/Cas9. *Cell Stem Cell* 2015;17:233–44. https://doi.org/10.1016/j.stem.2015.06.001
5. Bertero A, Pawlowski M, Ortmann D *et al.* Optimized inducible shRNA and CRISPR/Cas9 platforms for in vitro studies of human development using hPSCs. *Development* 2016;143:4405–18. https://doi.org/10.1242/dev.138081
6. Guzzardo PM, Rashkova C, dos Santos RL *et al.* A small cassette enables conditional gene inactivation by CRISPR/Cas9. *Sci Rep* 2017;7:16770. https://doi.org/10.1038/s41598-017-16931-z
7. Cassidy AM, Thomas DB, Kuliyev E *et al.* One-step generation of a conditional allele in mice using a short artificial intron. *Heliyon* 2022;8:e12630. https://doi.org/10.1016/j.heliyon.2022.e12630
8. Cassidy A, Pelletier S. CRISPR-Cas9-mediated insertion of a short artificial intron for the generation of conditional alleles in mice. *STAR Protocols* 2023;4:102116. https://doi.org/10.1016/j.xpro.2023.102116
9. Wu S-HS, Lee H, Szép-Bakonyi R *et al.* SCON—a Short Conditional intrON for conditional knockout with one-step zygote injection. *Exp Mol Med* 2022;54:2188–99. https://doi.org/10.1038/s12276-022-00891-0
10. Wu S-HS, Kim S, Lee H *et al.* Red2Flpe-SCON: a versatile, multicolor strategy for generating mosaic conditional knockout mice. *Nat Commun* 2024;15:4963. https://doi.org/10.1038/s41467-024-49382-y
11. McBeath E, Fujiwara K, Hofmann M-C. Evidence-based guide to using artificial introns for tissue-specific knockout in mice. *Int J Mol Sci* 2023;24:10258. https://doi.org/10.3390/ijms241210258
12. Koirala A, O'Connor K, Bare S *et al.* eSPLIT and iSWAP: cRISPR-mediated conditional allele engineering with short artificial introns. bioRxiv, https://doi.org/10.64898/2025.12.22.696077, 24 December 2025, preprint: not peer reviewed.
13. Walker C, Detrich HW, Westerfield M, Zon LI (eds.), *The Zebrafish: Genetics and Genomics*. San Diego, CA: Academic Press, 1998. Vol. 60, pp. 43–70.
14. Concordet J-P, Haeussler M. CRISPOR: intuitive guide selection for CRISPR/Cas9 genome editing experiments and screens. *Nucleic Acids Res* 2018;46:W242–5. https://doi.org/10.1093/nar/gky354
15. Varshney GK, Pei W, LaFave MC *et al.* High-throughput gene targeting and phenotyping in zebrafish using CRISPR/Cas9. *Genome Res* 2015;25:1030–42. https://doi.org/10.1101/gr.186379.114
16. Jao LE, Wente SR, Chen W. Efficient multiplex biallelic zebrafish genome editing using a CRISPR nuclease system. *Proc Natl Acad Sci USA* 2013;110:13904–9. https://doi.org/10.1073/pnas.1308335110
17. Hesselson D, Anderson RM, Beinat M *et al.* Distinct populations of quiescent and proliferative pancreatic β-cells identified by HOTcre mediated labeling. *Proc Natl Acad Sci USA* 2009;106:14896–901. https://doi.org/10.1073/pnas.0906348106
18. Horstick EJ, Jordan DC, Bergeron SA *et al.* Increased functional protein expression using nucleotide sequence features enriched in highly expressed genes in zebrafish. *Nucleic Acids Res* 2015;43:e48–. https://doi.org/10.1093/nar/gkv035
19. Kwan KM, Fujimoto E, Grabher C *et al.* The Tol2kit: a multisite gateway-based construction kit for Tol2 transposon transgenesis constructs. *Dev Dyn* 2007;236:3088–99. https://doi.org/10.1002/dvdy.21343
20. Hall TE, Martel N, Ariotti N *et al.* In vivo cell biological screening identifies an endocytic capture mechanism for T-tubule formation. *Nat Commun* 2020;11:3711. https://doi.org/10.1038/s41467-020-17486-w
21. Fenno LE, Mattis J, Ramakrishnan C *et al.* Targeting cells with single vectors using multiple-feature Boolean logic. *Nat Methods* 2014;11:763–72. https://doi.org/10.1038/nmeth.2996
22. Zhao C, Teng EM, Summers RG *et al.* Distinct morphological stages of dentate granule neuron maturation in the adult mouse hippocampus. *J Neurosci* 2006;26:3–11. https://doi.org/10.1523/JNEUROSCI.3648-05.2006
23. Ewels PA, Peltzer A, Fillinger S *et al.* The nf-core framework for community-curated bioinformatics pipelines. *Nat Biotechnol* 2020;38:276–8. https://doi.org/10.1038/s41587-020-0439-x
24. Martin M. Cutadapt removes adapter sequences from high-throughput sequencing reads. *EMBnet j* 2011;17:10–2. https://doi.org/10.14806/ej.17.1.200
25. Dobin A, Davis CA, Schlesinger F *et al.* STAR: ultrafast universal RNA-seq aligner. *Bioinformatics* 2012;29:15–21. https://doi.org/10.1093/bioinformatics/bts635

26. Patro R, Duggal G, Love MI *et al.* Salmon provides fast and bias-aware quantification of transcript expression. *Nat Methods* 2017;14:417–9. https://doi.org/10.1038/nmeth.4197
27. Soneson C, Love M, Robinson M. Differential analyses for RNA-seq: transcript-level estimates improve gene-level inferences [version 2; peer review: 2 approved]. *F1000Res* 2016;4:1521, https://doi.org/10.12688/f1000research.7563.2 .
28. Robinson MD, McCarthy DJ, Smyth GK. edgeR: a Bioconductor package for differential expression analysis of digital gene expression data. *Bioinformatics* 2009;26:139–40. https://doi.org/10.1093/bioinformatics/btp616
29. Kim H, Heo S-Y, Kim Y-I *et al.* Diverse bat organoids provide pathophysiological models for zoonotic viruses. *Science* 2025;388:756–62. https://doi.org/10.1126/science.adt1438
30. Koo B-K, Spit M, Jordens I *et al.* Tumour suppressor RNF43 is a stem-cell E3 ligase that induces endocytosis of Wnt receptors. *Nature* 2012;488:665–9. https://doi.org/10.1038/nature11308
31. Sato T, Vries RG, Snippert HJ *et al.* Single Lgr5 stem cells build crypt-villus structures in vitro without a mesenchymal niche. *Nature* 2009;459:262–5. https://doi.org/10.1038/nature07935
32. Merenda A, Andersson-Rolf A, Mustata RC. *et al.* A protocol for multiple gene knockout in mouse small intestinal organoids using a CRISPR-concatemer *J Vis Exp* 2017;55916.
33. Martin FJ, Amode MR, Aneja A *et al.* Ensembl 2023. *Nucleic Acids Res* 2022;51:D933–41. https://doi.org/10.1093/nar/gkac958
34. Labun K, Montague TG, Krause M *et al.* CHOPCHOP v3: expanding the CRISPR web toolbox beyond genome editing. *Nucleic Acids Res* 2019;47:W171–4. https://doi.org/10.1093/nar/gkz365
35. Letunic I, Bork P. Interactive Tree Of Life (iTOL) v5: an online tool for phylogenetic tree display and annotation. *Nucleic Acids Res* 2021;49:W293–6. https://doi.org/10.1093/nar/gkab301
36. Rodriguez JM, Pozo F, Cerdán-Vélez D *et al.* APPRIS: selecting functionally important isoforms. *Nucleic Acids Res* 2021;50:D54–9. https://doi.org/10.1093/nar/gkab1058
37. Crooks GE, Hon G, Chandonia J-M *et al.* WebLogo: a sequence logo generator. *Genome Res* 2004;14:1188–90. https://doi.org/10.1101/gr.849004
38. Miura H, Quadros RM, Gurumurthy CB *et al.* Easi-CRISPR for creating knock-in and conditional knockout mouse models using long ssDNA donors. *Nat Protoc* 2018;13:195–215. https://doi.org/10.1038/nprot.2017.153
39. Quadros RM, Miura H, Harms DW *et al.* Easi-CRISPR: a robust method for one-step generation of mice carrying conditional and insertion alleles using long ssDNA donors and CRISPR ribonucleoproteins. *Genome Biol* 2017;18:92. https://doi.org/10.1186/s13059-017-1220-4
40. Camp EL,M. Tyrosinase gene expression in zebrafish embryos. *Dev Genes Evol* 2001;211:150–3. https://doi.org/10.1007/s004270000125
41. Cao S, Dong Z, Dong X *et al.* Zebrafish sox2 is required for the swim bladder inflation by controlling the swim-up behavior. *Zebrafish* 2023;20:10–8. https://doi.org/10.1089/zeb.2022.0043
42. Okuda Y, Yoda H, Uchikawa M *et al.* Comparative genomic and expression analysis of group B1 sox genes in zebrafish indicates their diversification during vertebrate evolution. *Dev Dyn* 2006;235:811–25. https://doi.org/10.1002/dvdy.20678
43. Chaterji S, Ahn EH, Kim D-H. CRISPR genome engineering for human pluripotent stem cell research. *Theranostics* 2017;7:4445–69. https://doi.org/10.7150/thno.18456
44. Li X-L, Li G-H, Fu J *et al.* Highly efficient genome editing via CRISPR–Cas9 in human pluripotent stem cells is achieved by transient BCL-XL overexpression. *Nucleic Acids Res* 2018;46:10195–215. https://doi.org/10.1093/nar/gky804
45. Xiao W, Adhikari S, Dahal U *et al.* Nuclear m6A Reader YTHDC1 regulates mRNA splicing. *Mol Cell* 2016;61:507–19. https://doi.org/10.1016/j.molcel.2016.01.012
46. Liu J, Gao M, He J *et al.* The RNA m6A reader YTHDC1 silences retrotransposons and guards ES cell identity. *Nature* 2021;591:322–6. https://doi.org/10.1038/s41586-021-03313-9
47. Zhuang W, Ye T, Wang W *et al.* CTNNB1 in neurodevelopmental disorders. *Front Psychiatry* 2023;14:1143328.
48. Andersson-Rolf A, Mustata RC, Merenda A *et al.* One-step generation of conditional and reversible gene knockouts. *Nat Methods* 2017;14:287–9. https://doi.org/10.1038/nmeth.4156
49. Kim HK, Lee S, Kim Y *et al.* High-throughput analysis of the activities of xCas9, SpCas9-NG and SpCas9 at matched and mismatched target sequences in human cells. *Nat Biomed Eng* 2020;4:111–24. https://doi.org/10.1038/s41551-019-0505-1
50. Sugimoto K, Hui SP, Sheng DZ *et al.* Dissection of zebrafish shha function using site-specific targeting with a Cre-dependent genetic switch. *eLife* 2017;6:e24635. https://doi.org/10.7554/eLife.24635
51. Liu F, Kambakam S, Almeida MP *et al.* Cre/lox regulated conditional rescue and inactivation with zebrafish UFlip alleles generated by CRISPR-Cas9 targeted integration. *eLife* 2022;11:e71478. https://doi.org/10.7554/eLife.71478
52. Hans S, Zöller D, Hammer J *et al.* Cre-Controlled CRISPR mutagenesis provides fast and easy conditional gene inactivation in zebrafish. *Nat Commun* 2021;12:1125. https://doi.org/10.1038/s41467-021-21427-6
53. Aksoy YA, Nguyen DT, Chow S *et al.* Chemical reprogramming enhances homology-directed genome editing in zebrafish embryos. *Commun Biol* 2019;2:198. https://doi.org/10.1038/s42003-019-0444-0
54. Zhang Y, Zhang Z, Ge W. An efficient platform for generating somatic point mutations with germline transmission in the zebrafish by CRISPR/Cas9-mediated gene editing. *J Biol Chem* 2018;293:6611–22. https://doi.org/10.1074/jbc.RA117.001080
55. Boel A, De Saffel H, Steyaert W *et al.* CRISPR/Cas9-mediated homology-directed repair by ssODNs in zebrafish induces complex mutational patterns resulting from genomic integration of repair-template fragments. *Dis Models Mech* 2018;11:dmm035352. https://doi.org/10.1242/dmm.035352

Received: September 23, 2025. **Revised:** April 17, 2026. **Accepted:** April 21, 2026